

COMPREHENSIVE REVIEW

Mathematical and computational modeling of fats and triacylglycerides

Robert J. Cordina^{1,2}  | Beccy Smith¹ | Tell Tuttle²

¹Cadbury UK Ltd., Birmingham, UK

²Department of Pure and Applied Chemistry, University of Strathclyde, Glasgow, UK

Correspondence

Tell Tuttle, Department of Pure and Applied Chemistry, University of Strathclyde, 295 Cathedral Street, Glasgow G1 1XL, UK. Email: tell.tuttle@strath.ac.uk

Abstract

Fats and oils are found in many food products; however, their macroscopic properties are difficult to predict, especially when blending different fats or oils together. With difficulties in sourcing specific fats or oils, whether due to availability or pricing, food companies may be required to find alternative sources for these ingredients, with possible differences in ingredient performance. Mathematical and computational modeling of these ingredients can provide a quick way to predict their properties, avoiding costly trials or manufacturing problems, while, most importantly, keeping the consumers happy. This review covers a range of mathematical models for triacylglycerides (TAGs) and fats, namely, models for the prediction of melting point, solid fat content, and crystallization temperature and composition. There are a number of models that have been designed for both TAGs and fats and which have been shown to agree very well with empirical measurements, using both kinetic and thermodynamic approaches, with models for TAGs being used to, in turn, predict fat properties. The last section describes computational models to simulate the behavior of TAGs using molecular dynamics (MD). Simulation of TAGs using MD, however, is still at an early stage, although the most recent papers on this topic are bringing this area up to speed.

KEYWORDS

kinetics, molecular dynamics, solid fat content, solid–liquid equilibria, thermodynamics

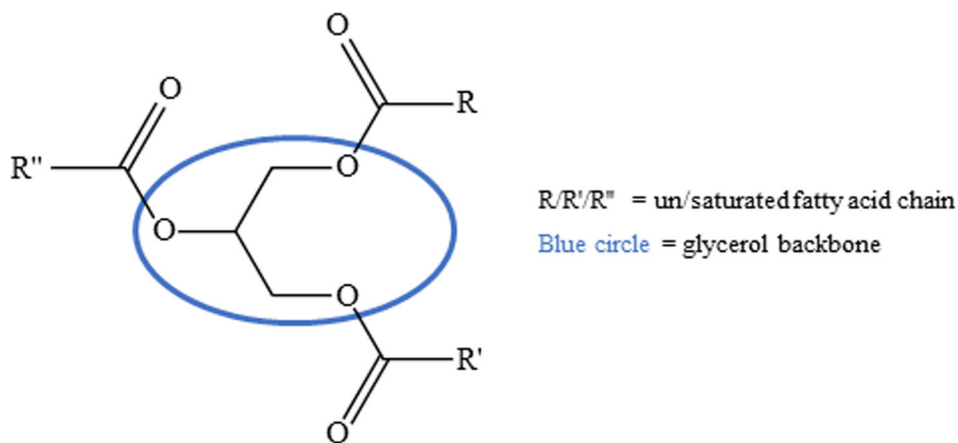
1 | INTRODUCTION

Fats and oils are used extensively in the food industry (Gunstone, 2008). The physical properties of these fats and oils, such as their melting range and solid fat content (SFC) profile, will have a big impact on both their processability and their eating characteristics (Devi & Khatkar, 2016). A fat that has a waxy “tail”, that is, a fat that has constituent

triacylglycerides (TAGs—Figure 1) that melt at a temperature higher than body temperature and which, hence, feel waxy in the mouth, may be unpleasant to consumers. Conversely, a fat that starts to crystallize only at very low temperatures may result in a product that feels very oily for the consumer. These properties could also have an effect on processing, with fats which crystallize even at relatively high temperatures possibly causing issues with build-up

This is an open access article under the terms of the [Creative Commons Attribution-NonCommercial](https://creativecommons.org/licenses/by-nc/4.0/) License, which permits use, distribution and reproduction in any medium, provided the original work is properly cited and is not used for commercial purposes.

© 2024 The Authors. *Comprehensive Reviews in Food Science and Food Safety* published by Wiley Periodicals LLC on behalf of Institute of Food Technologists.



Examples of fatty acid chains:

Lauric	C12:0	saturated 12-carbon chain (including carbonyl C)
Palmitic	C16:0	saturated 16-carbon chain
Stearic	C18:0	saturated 18-carbon chain
Oleic	<i>cis</i> -C18:1 ω 9	<i>cis</i> -unsaturated 18-carbon chain with unsaturation at C-9
Linoleic	<i>cis</i> -C18:2 ω 6	<i>cis</i> -unsaturated 18-carbon chain with unsaturation at C-9 and C-12
Elaidic	<i>trans</i> -C18:1 ω 9	<i>trans</i> -unsaturated 18-carbon chain with unsaturation at C-9

FIGURE 1 Triacylglyceride structure and examples of fatty acid chains.

in the equipment being used, eventually causing clogging issues (Devi & Khatkar, 2016; Ehlers, 2012).

The food industry, thus, faces a number of challenges when sourcing and using new fats and oils; they must be amenable to easy processing, and they must perform well in the products that they are going to be used in. In addition to these requirements, they generally also have to be nutritionally acceptable (which is usually taken to mean lower in saturated fat and with no or very little *trans* fat content) (Dhaka et al., 2011; Talbot, 2016) and, increasingly, obtained from sustainable sources (Novelli, 2016). The former two criteria are generally satisfied by the macroscopic properties of the fats and oils, such as the SFC profile. The requirement for fats with a lower saturation content and no *trans* fat is, however, satisfied only by the molecular structure of the constituent TAGs in any fat or oil, namely, the number and type (*cis* or *trans*) of double bonds on the fatty acid (FA) chains. Although the amount of *trans* FAs found in unmodified fats is minimal, this increases significantly with partial hydrogenation of the fats (Farr et al., 2005; Mensink et al., 2016). Partial hydrogenation is used to change the macroscopic physical properties of the fats by changing the molecular structure; however, due to the detrimental effects on health of *trans* fats, these are being used increasingly less often. This has led companies to use interesterified fats, where the individual FA structure is

unchanged, but the position of the FA chains on the TAGs' glycerol backbone is. This leads to different macroscopic properties of both the individual TAGs produced and the bulk fat, which, however, may not be immediately obvious at the start (Mensink et al., 2016). Thus, having mathematical and computational tools that can predict the properties of both the TAGs and the fat saves a lot of time for people working in these industries.

The food industry also faces other, global, challenges, such as sourcing and sustainability. Increasingly, supply chain issues due to global events are leading to difficulties in sourcing a specific fat or oil (Ben Hassen & El Bilali, 2022; Glauben et al., 2022), which leads to companies having to source alternative ingredients that may not perform in the same exact manner as the fat or oil being replaced. A solution to this is to blend two or more fats or oils to achieve the same macroscopic properties; however, fats and oils commonly do not show linearity when blended, that is, a 50:50 blend of two fats will not have properties exactly mid-way between the constituent fats (Timms, 1984). Thus, a number of trials are required to test out the new blends, which can lead to delays in product development and manufacturing until a blend that satisfies the company's criteria is found.

With an ever-increasing focus on sustainability, a number of companies are working on the development of

lab-grown fats and oils. This entails either using microorganisms, such as yeasts or bacteria, to ferment or metabolize feed nutrients to produce TAGs, which can be then purified and used as a fat or oil, or using cell culture propagation, where cells taken from natural sources are grown in a lab with the aim of producing fats and oils that are similar to that extracted from the botanical or animal source (Eibl et al., 2021; Schirmer et al., 2022; Zagury et al., 2022). In any case, any such fats and oils need to have the right physical properties to be used by food manufacturers, meaning that the constituent TAGs must have the desired molecular structure, and the TAGs must be in the correct proportions to give the desired macroscopic fat properties.

The physical properties of a fat/oil are dependent on the structure and the ratio of the constituent TAGs making up the fat/oil. This means that fats with TAGs with the same constituent FA chains, but positioned differently on the glycerol backbone, will have different physical properties. Hence, whether it is changing a TAG's positional structure through enzymatic interesterification, lab-grown fats that can be tuned to produce the right proportions of TAGs, or blending of native fats and oils, having the right physical properties is crucial for acceptance by both the food manufacturers and their consumers. Thus, being able to predict the physical properties of these fats, or, ideally, being able to find the right TAG profile that would achieve the desired macroscopic physical characteristics, would result in significant time and cost savings. The most efficient manner of predicting the properties would be through mathematical and computational approaches—this review covers the main tools available for such purposes.

2 | CALCULATION OF THERMODYNAMIC PROPERTIES OF PURE TAGS

TAGs are composed of three (*tri*) FA chains (*acyl*), which are esterified to a glycerol (*glyceride*) backbone (Figure 1). TAGs, thus, have a very similar chemical structure to one another, with the main differences being the length of the FA chain, the number and type (*cis* or *trans*) of double bonds on the chain, if any, and the position of the FAs on the glycerol backbone. These differences have an impact on their macroscopic properties, including melting temperature (T_m) and enthalpy of fusion (ΔH_f) (or melting enthalpy). It is known that, as with *n*-alkanes, the longer the FA chains, the higher the T_m and ΔH_f . It is, however, not as straightforward as that, as this only really applies for saturated TAGs (Seilert & Flöter, 2021).

When comparing TAGs with the same carbon number, the presence of double bonds lowers the T_m and ΔH_f when compared to the TAG with no unsaturation. The type of

double bond also has an impact, with *trans* double bonds having a lower impact. One example that could be mentioned is the comparison of tristearin (with three C18:0 FA chains), trielaidin (with three *trans*-C18:1 ω 9 FA chains), and triolein (with three *cis*-C18:1 ω 9 FA chains). The T_m of these three TAGs decreases drastically from tristearin to trielaidin to triolein (72.5, 42.2, and 4.8°C, respectively), with a corresponding decrease in ΔH_f (T_m and ΔH_f values obtained online from the Tri(acyl)glyceride Property Calculator (TPC) (Moorthy et al., 2016, 2017) for the β polymorph in all cases). It is thus very clear that the presence and type of a single double bond on each of the chains is having a large impact. The energy required to melt out the crystal structures is decreasing, even between tristearin and trielaidin, which are known to have similar double-chain length, triclinic crystal structures in the β form with fully parallel FA chains (Culot et al., 2000; Van Langevelde et al., 2001). Moreover, the position of the double bond has also been shown to have an impact on the ΔH_f value, with no clear trend between the position of a single double bond and ΔH_f (Timms, 1978).

TAGs are also known to be polymorphic (with the three most commonly known polymorphs referred to, in increasing order of thermodynamic stability, as α , β' , and β , although there may be other polymorphs). A number of TAGs are also known to have sub-polymorphs (e.g., in decreasing order of thermodynamic stability, β_1 , β_2 , etc.) (Ghazani & Marangoni, 2018; Ghazani & Marangoni, 2023; Peschar et al., 2006; van Mechelen et al., 2006). This means that, even though they are all β polymorphs, that is, being in a similar specific crystal structure (generally triclinic for β polymorphs), there are still some small differences between them.

All this means that being able to predict the difference in thermodynamic properties between different, but similar, structures and between polymorphs, or even sub-polymorphs, is not straightforward as there are many complexities that need to be taken into consideration. This paper discusses the main mathematical modeling approaches that have been proposed.

2.1 | Early attempts to predict thermodynamic properties

Over the years, there have been a number of studies that have attempted to build mathematical models to predict thermodynamic properties of TAGs, namely, the melting temperature, the enthalpy of fusion, and the entropy of fusion (ΔS_f). Given the relationship between temperature (T), enthalpy (H), and entropy (S) as described in the Gibbs energy (G) equation ($\Delta G = \Delta H - T\Delta S$), and the fact that in a system at equilibrium (such as a system held at the

melting temperature), $\Delta G = 0$, if any two of the other terms can be predicted, then the third term is easily determined by a simple equation rearrangement.

The earlier models were based on the total number of carbons present in the three FA chains of the TAG, which meant that the predicted properties of TAGs with the same set of FA chains bonded to different glycerol positions would be the same, which is known to be incorrect, even for fully saturated systems (Garti & Widlak, 2012).

A study by Zacharis (1977) proposed a linear model to predict the melting temperature based on the number of carbon atoms on the FA chains, using the following equation:

$$TN = C_0 + T_\infty N \quad (1)$$

where T is the melting temperature and N is the number of long-chain carbon atoms, whereas C_0 and T_∞ were determined from linear regression of a TN versus N plot. The model was used to determine the coefficients for different polymorphs. This was, however, limited to fully saturated TAGs with three identical FA chains.

Shortly after, Timms (1978) proposed a model to predict ΔH_f (kcal/mol) for mixed (different FA chains) saturated and unsaturated TAGs, again using linear equations based on the total number of carbon atoms in the FA chains as shown in the following equations:

$$\Delta H_f^\beta = 1.023 (\text{Carbon number}) - 7.79 \quad (\text{general equation}) \quad (2)$$

$$\Delta H_f^\beta = 1.023 (\text{Carbon number}) - 7.79 - 4.3 \quad (3)$$

(for asymmetric, saturated and transTAGs)

$$\Delta H_f^{\beta'} = 0.76 \Delta H_f^\beta \quad (4)$$

To compensate for the fact that saturated and unsaturated FA chains may have the same number of carbons, an effective carbon number for unsaturated chains was given by the author. For example, although the carbon number for stearic acid is 18, the effective carbon numbers for oleic, linoleic, and elaidic acids were given as 10.4, 8.9, and 14.0, respectively, despite all these FAs consisting of 18 carbons (Figure 1). In this case, the different numbers reflect either the increased saturation of the chain (increasing from linoleic (8.9) to oleic (10.4) to stearic (18)) or the *cis*-/*trans*-configuration of the double bond (with the effective carbon number for elaidic acid (14.0) being higher than that for oleic acid (10.4)), indicating the different degree of interaction due to the different structures and, hence, different molecular packing in the crystals (Timms, 1978).

A later model by Ollivon and Perron (1982) determined parameters to predict the thermodynamic properties using simple linear fit equations of the type $y = an + b$, where n is the total carbon number of the FA chains. The empirical correlations to predict ΔH_f (kJ/mol) for the α , β' , and β polymorphs of fully saturated TAGs are given in the following equations:

$$\Delta H_f^\alpha = 2.5n - 27.5 \quad (5)$$

$$\Delta H_f^{\beta'} = 3.87n - 19.2 \quad (6)$$

$$\Delta H_f^\beta = 4.20n - 29.9 \quad (7)$$

However, the ΔH_f for unsaturated TAGs was calculated from the value of ΔH_f for saturated TAGs with the same carbon number, less a contribution from the double bonds, as per the following equation:

$$\Delta H_{f,unsat} = \Delta H_{f,sat} - 115 (1 - e^{-0.706\Delta}) \quad (8)$$

where Δ is the number of double bonds in the TAG. A limitation of this study was that the relationships were developed for TAGs with three identical FA chains.

These models, while being simple and easy to use, all have the same drawbacks, namely, the predictions are the same irrespective of the position of the FA chains on the glycerol backbone, they only predict one thermodynamic property (T_m or ΔH_f), which means that one cannot determine all three thermodynamic properties (T_m , ΔH_f , and ΔS_f) at melting (i.e., when $\Delta G = 0$), and they all require empirical measurements in order to obtain the regression parameters.

2.2 | Model refinement—going from simple linear empirical models to structure-based models

Most of the limitations described in the section above were overcome in the seminal work by Wesdorp (1990) (which was then republished in 2013 (Marangoni & Wesdorp, 2013) and in 2016 (Moorthy et al., 2016), and then re-parameterized in 2021 (Seilert & Flöter, 2021)) and in another model by Zéberg-Mikkelsen and Stenby (1999).

The Wesdorp model is a semiempirical model to predict T_m and ΔH_f for both saturated and unsaturated TAGs as a function of the total number of carbons in the FA chains, the degree of saturation of the chains, and the differences between the chain lengths. A number of

equation modifiers account for TAGs with different FA chains, odd-numbered chains, and unsaturated TAGs. This model, thus, has one crucial difference from the other models, with both the different FA chain lengths and their position on the glycerol backbone being part of the model, thus being able to predict different thermodynamic properties for TAGs with the same FA chains but at different positions. This is introduced into the model by the simple calculation of two values, x and y , where x is the difference between the shortest chain length in positions 1 or 3 and the chain length at position 2, and y is the difference in chain length between the chains at positions 1 and 3. In this case, the model actually predicts ΔH_f and ΔS_f , with T_m then being predicted using a Taylor series expansion as a function of the inverse of the total carbon number, which results in two parameters that need to be determined in an equation similar to that used by Zacharis (1977). The value of these parameters was estimated using two approaches; the first approach is a quadratic estimation based on the chain length differences, and the second is based on the principle that, at equilibrium, T_m of a pure component is equal to the ratio of ΔH_f and ΔS_f (see Seilert et al. (2021) for an excellent summary of all the parameters and equations used in this model). This model introduced a lot of predictive power; however, it has one distinguishing feature in that some of the model predictions lack thermodynamic consistency. This means that the predicted T_m and ΔH_f does not always increase with the increasing thermodynamic stability of different polymorph for any given TAG (Moorthy et al., 2016; Seilert et al., 2021; Wesdorp, 1990). This model is, however, still considered one of the best models available to users and is easily accessed online via the TPC (Moorthy et al., 2016, 2017).

The Zéberg-Mikkelsen and Stenby model uses a group contribution method, where the parameters used in the model describe the interaction of the median FA chain to the terminal FA chains as well as the “class” of the TAG, that is, how many FA chains are identical, and the position of the identical FA chains, giving four possible classes. These classes are defined as *III* (three identical FA chains), *IJJ* (two identical FA chains at glycerol positions 1 and 2, i.e., $I \neq J$), *IJI* (two identical FA chains at glycerol positions 1 and 3), and *IJK* (three different FA acid chains). The general equations used in this model are as follows:

$$T_m \text{ (K)} = K_{T,IJK} \left(\sum T_{IJ} \right) \quad (9)$$

$$\Delta H_f \text{ (kJ/mol)} = K_{H,IJK} \left(\sum H_{IJ} \right) \quad (10)$$

where I and K refer to the terminal FA chains (i.e., the FA chains at glycerol positions 1 and 3), J refers to the FA chain at glycerol position 2, $K_{T,IJK}$ and $K_{H,IJK}$ are the TAG class

parameters (for any class), and T_{IJ} and H_{IJ} are the group interaction parameters. The equations can be applied to any polymorph; however, the parameter values differ for the respective polymorphs. In this model, the parameters were estimated by minimization of the squares of the difference between the experimental and predicted values of T_m and ΔH_f , making it (similar to the Wesdorp (1990) and Seilert et al. (2021) models) a semiempirical model, albeit one with more granularity than the older models.

When comparing the predictive accuracy of this model to those of Wesdorp (1990), Ollivon and Perron (1982), and Timms (1978), this model performed the best. It is, however, restricted by being only applicable to TAGs with FA chains for which the pairwise-interaction parameters are known, as well as being developed only for saturated TAGs, whereas Wesdorp's (1990) model does not have these limitations.

One of the main factors impacting the accuracy of any semiempirical model is the quality of the data used to estimate the value of the parameters used in the model. Data accuracy can be affected by both the measurement technique and the sample purity, and further compounded by the fact that TAGs, especially unsaturated ones, can be found in different polymorphic forms with different chain length structures (Seilert et al., 2021). To resolve for this, the 2021 study by Seilert et al. revisited the Wesdorp model, where the model was also re-parameterized using a reduced dataset that contained only thermodynamically consistent data gathered from a number of other published studies, a good number of which are more recent than the initial 1990 Wesdorp study. The authors found that T_m and ΔH_f predictions for saturated TAGs were found to be thermodynamically consistent without the need for additional thermodynamic constraints during the parameter fitting, with the effect of using either the reduced or the full dataset being small. However, the predictive power for unsaturated TAGs was deemed to be significantly reduced. The main reason given for this was the quantity of data available for the parameter estimation. The authors suggest that a larger unsaturated TAG dataset would be required to overcome the lack of thermodynamic consistency. On the other hand, using the reduced dataset gave a parameter set with increased consistency.

This study was quickly followed by another from the same group (Seilert & Flöter, 2021). This model, while still predicting T_m and ΔH_f for pure (single) TAGs, uses less than half the number of parameters compared to the Wesdorp model, while surpassing the same model on prediction quality and thermodynamic consistency, with the latter not only for the ΔH_f prediction but also including (in most cases) the estimated parameters too. To use this model an understanding of the crystalline structure of the TAG is required, especially whether the

TAGs are arranged in double chain length or triple chain length configuration, and their polymorph (α , β' , or β). The prediction of ΔH_f is based on the following structural information; an interaction parameter A (which is a function of the un/saturation and position of the different FAs), the angle of tilt τ (which is different depending on the polymorph), the average lateral distance d (which, again, is different for the different polymorphs), the characteristic carbon number C in the reference cell leaflet, a parameter g which is dependent on whether the glycerol backbone is in a chair or tuning form conformation, whereas two other parameters (c and a) account for the methyl end plane interactions, which in turn depend on the differences in lengths of the different FA chains and the inclination of the chains in the different polymorphs (Scheme 1).

All of these terms were included after considering that ΔH_f is a function of the enthalpies of the interaction between the FA chains, the contribution of the glycerol backbone, and the interactions at the methyl end plane of the TAGs. Thus, all the parameters used in this model have physical meaning and are not simply a means of fitting empirical data. In this model T_m is predicted using the predicted value of ΔH_f and an empirically determined linear relationship between ΔS_f and ΔH_f . This linear relationship was determined from published data for n -alkanes and other related homologous alkyl-series, which is also valid for saturated monoacid TAGs. The authors state that determination of ΔS_f from published ΔH_f and T_m data showed that the same linear $\Delta S_f/\Delta H_f$ relationship still held for mixed TAGs and unsaturated TAGs, and surprisingly even different polymorphs of the same TAG (Seilert & Flöter, 2021).

In summary, over the years, the models to predict the thermodynamic properties of TAGs have improved considerably, with some of the newer models making use of and refining some of the other older models. As can be seen in Table 1, the models have become applicable to a wider range of TAG types, for example, different polymorphs, un/saturation, FA asymmetry, and the position and length of the individual FA chains.

All of these models, however, are still empirical, or semiempirical, models, with a number of parameters needing to be fitted. Given that this is done by a comparison of the predicted values with empirical values, having accurate data is crucial. With different values being reported in different papers or with data simply not available, this is no easy task.

This is further complicated by the fact that new sub-polymorphs of pure TAGs may be found. Two examples are the discovery in 2018 of two new β polymorphs of 1-palmitoyl-2-oleoyl-3-stearoyl glycerol (Ghazani & Marangoni, 2018) and in 2023 of a new triclinic polymorph of tristearin, meaning that there are now two known β

polymorphs of this TAG (Ghazani & Marangoni, 2023), with each polymorph having a different T_m and ΔH_f , even though they are all classified as being in the triclinic β structure (they are generally denoted as β_1 , β_2 , etc., with the higher the number, the higher the T_m and ΔH_f). On the other hand, the models described above do not distinguish between these β sub-polymorphs, and hence they are currently inadequate to predict the difference in the thermodynamic properties between them.

3 | PREDICTION OF SOLID FAT CONTENT AND SOLID-LIQUID PHASE EQUILIBRIA OF TAG MIXTURES

Although the models to predict the thermodynamic properties of pure TAGs have proven very useful for research purposes, fats are composed of a blend of TAGs, which could run into tens of TAGs for a single fat. Moreover, fats, due to the inherent different thermodynamic properties of the different TAGs making up those fats, do not exhibit a sharp melting point but melt over a temperature range. Studies have shown that even relatively simple binary TAG systems show nonlinear behavior (Bayés-García et al., 2013; Smith et al., 2013; Zhang et al., 2018).

The SFC profile (a plot of SFC vs. temperature) is a crucial property of any fat as this directly impacts both the processing and eating properties of the fat and is hence important to both the manufacturer and the consumer. Given the nonlinear behavior of TAG mixtures, building a model to predict the melting behavior of a multi-TAG component fat system (i.e., not only the melting temperature range but also the SFC at any temperature within that range) is very challenging as any such model needs to take into consideration not only the presence of each component TAG but also the relative ratio of each TAG and their respective properties.

3.1 | Empirical regression models

Multiple groups have attempted to build models to predict liquid-solid equilibria for fats and oils, with most of these being based on empirical data, which is then used for finding correlations using regression or neural networks. For example, the study by Block et al. (1997), using neural networks to determine the optimal ternary fat blend to achieve the desired SFC profile, gave very good results, that is, the predicted SFC curve compared very well to the empirically determined SFC curve. This type of model, however, has the drawback that it is based on empirical data, that is, the SFC curves of other ternary blends made from the same three fats must be known before building the neural network, thus, not only requiring experimental

SCHEME 1 Model equations to predict T_m and ΔH_f based on a triacylglyceride (TAG)'s crystalline structure (Seilert & Flöter, 2021).

$$\text{DCL: } \Delta H_f^{\{k\}} = \frac{A}{d^{\{k\}6}} C + g^{\{k\}} (1 + g_{if} f_{if}) + c^{\{k\}} \sum_{i=1}^3 \tanh\left(\left(\sin \tau^{\{k\}} \frac{CLM_i}{C}\right)^{a^{\{k\}}}\right)$$

$$\text{TCL: } \Delta H_{f,tr}^{\{k\}} = \frac{1}{3} \frac{A_{middle}}{d^{\{k\}6}} C_{middle} + \frac{2}{3} \frac{A_{outer}}{d^{\{k\}6}} C_{outer} + g_{tr}^{\{k\}} (1 + g_{if} f_{if}) +$$

$$c_{tr}^{\{k\}} \tanh\left(\left(\sin \tau^{\{k\}} \frac{CLM_{tr}}{C_{outer}}\right)^{a_{tr}^{\{k\}}}\right)$$

For DCL:

if TAG = fully saturated; $A = A_{SS}$

if TAG = fully unsaturated; $A = A_{UU}$

if TAG = mix of saturated/unsaturated fatty acids

$$A = w_1 A_{SS} + w_2 A_{SU} (1 + p_E f_E + p_l f_l + p_{le} f_{le}) + (1 - w_1 - w_2) A_{UU} (1 + p_E f_E + p_l f_l + p_{le} f_{le})$$

For TCL:

$$A_{middle} = A_{UU,middle} (1 + p_{E,middle} f_{E,middle} + p_{l,middle} f_{l,middle} + p_{le,middle} f_{le,middle})$$

$$A_{outer} = A_{UU,outer} (1 + p_{E,outer} f_{E,outer} + p_{l,outer} f_{l,outer} + p_{le,outer} f_{le,outer})$$

Legend:

DCL	double chain-length crystal configuration
TCL	triple chain-length crystal configuration
{k}	α , β' , and β
Tr	ΔH_f calculated for TAGs in a TCL structure
C	characteristic carbon number in each leaflet
T	angle of tilt (90°, 70°, and 60° for α , β' , and β polymorphs, respectively)
g, g_{tr} , g_{if}	fitted glycerol backbone contributions
c, a	fitted methyl-end plane contributions
D	average lateral distance (4.79, 4.72, and 4.63 Å for α , β' , and β polymorphs, respectively)
CLM	chain length mismatch
A	interaction parameter
A_{SS} , A_{SU} , A_{UU}	fitted interaction parameters
w_1 , w_2	weights determined by combinatorics
	($w_1 = 1/9$ for SSU/SUS/USS TAGs, or $= 4/9$ for SUU/UUS/USU TAGs; $w_2 = 4/9$)
p_E , p_l , p_{le}	parameters to account for elaidic, linoleic, and linolenic fatty acids
f_E , f_l , f_{le}	switch functions (=1, if elaidic, linoleic, and linolenic fatty acids are present, respectively, otherwise = 0)
S	saturated fatty acid
U	unsaturated fatty acid
x, y	linear regression parameters of a plot ΔS_f vs. ΔH_f

At melting:

$$\Delta G = 0 =$$

$$\Delta H_f - T_m \Delta S_f$$

$$T_m = \frac{\Delta H_f}{\Delta S_f}$$

$$\text{with } \Delta S_f = x \Delta H_f + y$$

$$\Rightarrow T_m = \frac{\Delta H_f}{x \Delta H_f + y}$$

data to build the model but also limiting it to interpolation within the component fats being used to build the model (making it a “response surface” type model), and hence not being able to use a new component fat. The regression models by Augusto et al. (2012) also show excellent agreement with empirical results; however, these only show that various mathematical representations (in this case three sigmoidal functions, namely, Gompertz, power, and logistic models) can reproduce the empirically determined SFC curve of different fats accurately. Given that in each case the parameters were fitted for each fat, these mathemati-

cal representations provide no predictive power for other fats or blends of fats.

3.2 | Thermodynamic approaches to predicting fat SFC profiles

3.2.1 | Using thermodynamic properties only

Purely empirical models, such as those described in the previous section, require extensive empirical testing and

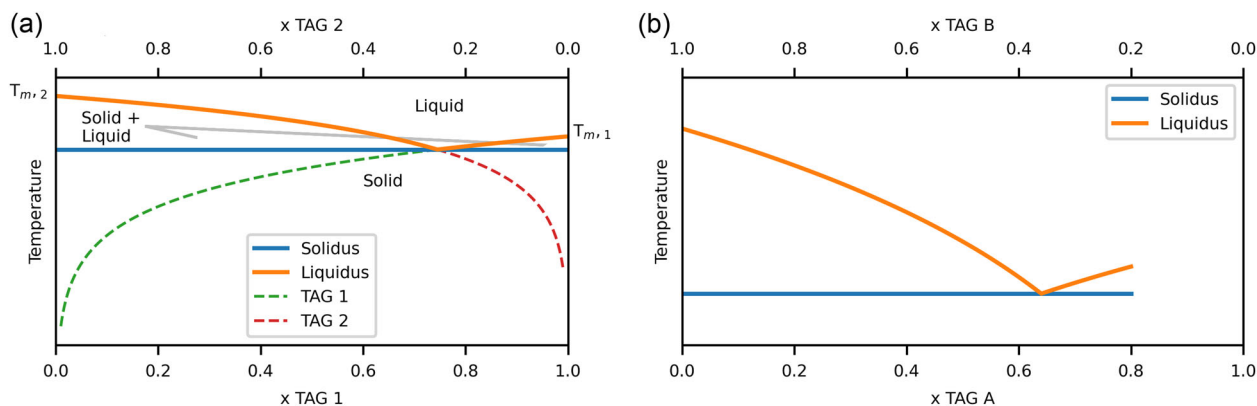


FIGURE 2 (a) Phase diagram sample built using the Hildebrand equation. (b) Determination of the solidus temperature of a binary triacylglycerides (TAG) system in a 3-component system, where the mole fraction of TAG C is kept constant at 0.2 (Schaink, 2023).

data gathering, and do not provide predictive power outside of the knowledge space built during that exercise. Taking a first principles approach and basing the models on thermodynamic theory and properties should give a much more flexible model that, in theory, could be applied to any fat/oil, or fat blend.

One of the simplest thermodynamic models that can be applied to describe the phase behavior of a mixture is the following Hildebrand equation (Hildebrand, 1929):

$$\ln(x_i) = \frac{\Delta H_{f,i}}{R} \left(\frac{1}{T_{m,i}} - \frac{1}{T} \right) \quad (11)$$

where x_i , $T_{m,i}$, and $\Delta H_{f,i}$ are the mole fraction in the liquid state, melting temperature (K), and enthalpy of fusion (J/mol) of TAG i , respectively, R is the universal gas constant (J/mol/K), and T (K) is the main variable. If the T_m and ΔH_f of the TAGs are known or are predicted as discussed in the previous section, and the Hildebrand equation is rearranged to calculate T , given that x_i can be varied from 0 to 1, a phase diagram of temperature versus mole fraction can be obtained very easily by taking the maximum value obtained at any given mole fraction, with the resulting line corresponding to the liquidus (the temperature at which the mixture is completely melted when heated, or conversely, the crystallization onset temperature when the mixture is cooled) (Figure 2a). It has to be noted that the Hildebrand equation assumes ideal behavior of the mixed liquid TAGs and no solid phase miscibility.

This method was recently extended by Schaink (2023) to multicomponent TAG systems, that is, fats. In this study, the author aimed to predict the SFC profile of a TAG mixture using only T_m and ΔH_f , that is, with no empirically fit parameters. Usually, when using the Hildebrand equation, a closure relation of $\sum_{i=1}^n x_i = 1$ is used. In the case of

Schaink's paper, this has been modified as $\sum_{i=1}^n x_i = 1 - x_{solvent} \neq 1$. This distinction is important as it considers any TAGs which are not crystallizing ($x_{solvent}$) at any given temperature as an inert liquid solvent. The approach taken is thus to calculate the liquidus curve using the Hildebrand model of each binary TAG system, that is, varying the mole fraction of any given two TAGs, while keeping the mole fraction of all other TAGs in the system constant (e.g., in a ternary system made up of TAGs A, B, and C in a 5:3:2 ratio, the mole fraction of TAG C is kept at 0.2, whereas the mole fractions of TAGs A and B are varied between 0 and 0.8, as shown in Figure 2b). Then, by assuming that the solidus temperature of that binary mixture is both equal to the minimum liquidus temperature and does not change with varying binary TAG ratio, the solidus temperature is obtained (Figure 2b).

The author then outlines that although the SFC of a multicomponent TAG mixture will be impacted by the solidus temperature of all the possible binary TAG mixtures, the SFC will be impacted to a greater degree by the solidus temperature of those binary TAG systems in which the component TAGs are present in a higher proportion. The relative contribution of each determined solidus temperature to the SFC at any given temperature is calculated as $\varphi_{i,j}$ (which is calculated as a function of the mole fractions), whereas the SFC is then calculated by summing the various $\varphi_{i,j}$ values at temperature T from the highest solidus temperature down to temperature T .

One important fact that this paper highlights is the impact of minor TAGs on fat behavior. For example, when modeling the SFC of cocoa butter using the three main component TAGs (POP, POSt, and StOSt) in a 26.3:50.6:23.1 ratio (a commonly used model system for cocoa butter), the resulting melting range was predicted to be at much higher

temperatures (in this case, the predicted melting range of this system in the β' polymorph was between approximately 34 and 36°C, whereas the empirical melting range was 10–35°C). However, when including six other minor TAGs in the predictive model, the predicted SFC profile was much close to the empirically determined profile.

It has to be underlined that this approach to modeling the SFC profile of any fat makes use of a model which does not require any empirically determined parameters if T_m and ΔH_f of the constituent TAGs are known. If these are not known they could be predicted from the Wesdorp (1990) or Zéberg-Mikkelsen and Stenby (1999) models, which would, however, mean that the model's success would again be dependent on accurate parameter estimation.

3.2.2 | Gibbs free energy calculations

In a system at equilibrium, such as a melting system, the chemical potential μ of each component in a mixture must be equal in both phases (Equation 12).

$$\mu_i^{solid} = \mu_i^{liquid} \quad (12)$$

This equation can be expressed in terms of the activity coefficients (γ), the mole fractions (x), temperature (T), and the universal gas constant (R) (Equation 13).

$$\mu_i^{0,S} + RT \ln(\gamma_i^S x_i^S) = \mu_i^{0,L} + RT \ln(\gamma_i^L x_i^L) \quad (13)$$

which can be further expressed as (Marangoni & Wesdorp, 2013; Prausnitz et al., 1999)

$$\ln\left(\frac{\gamma_i^S x_i^S}{\gamma_i^L x_i^L}\right) = \frac{\Delta H_{f,i}}{R} \left(\frac{1}{T} - \frac{1}{T_{m,i}}\right) \quad (14)$$

TAG mixtures do not behave as ideal solutions and hence will have an excess Gibbs energy g^E (the difference in the Gibbs free energy of an actual system from the same system behaving as an ideal solution). The Gibbs energy (G) (J/mol) of a phase is given in the following equation:

$$G = \sum_{i=1}^N n_i \mu_i = G^{ideal} + RT \sum_{i=1}^N n_i \ln \gamma_i \quad (15)$$

where R is the ideal gas constant (J/mol/K), T is temperature (K), and n and μ are the number of moles and the chemical potential of TAG i , respectively (Marangoni & Wesdorp, 2013; Prausnitz et al., 1999). The excess Gibbs

energy g^E is thus defined as the following equation:

$$g^E = G - G^{ideal} = RT \sum_{i=1}^N n_i \ln \gamma_i \quad (16)$$

If one has a model for g^E then the activity coefficient γ can be determined, which can then be used in Equation (14). This would leave only the mole fractions x_i^S and x_i^L as the unknown variables, which can then be computed, and hence determining the ratio of moles in the solid and liquid phases, that is, the SFC at any given temperature. This is however still nontrivial as there are two phases (solid and liquid, if assuming that the crystalline solid is only one polymorph) and the number of TAGs can run into tens per fat.

In a pure phase g^E must be equal to 0. The simplest model to describe this in a binary system is given in Equation (17). The presence of the $x_1 x_2$ term ensures that in a system made up of a single component, that is, as x_1 or $x_2 \rightarrow 0$, $g^E \rightarrow 0$ (i.e., an ideal solution).

$$g^E = A x_1 x_2 \quad (17)$$

Differentiating Equation (16) with respect to component i gives the following equation:

$$\frac{\partial n_T g^E}{\partial n_i} = \bar{g}_i^E = RT \ln \gamma_i \quad (18)$$

where n_i and n_T are the number of moles of TAG i and the total number of moles in the mixture respectively. Given that $n_i/n_T = x_i$, this results in Equation (19), known as the 2-suffix Margules equations (Margules, 1895).

$$RT \ln \gamma_1 = A x_2^2 \text{ and } RT \ln \gamma_2 = A x_1^2 \quad (19)$$

Extending this to a multicomponent system gives the following equations:

$$g^E = \sum_i^n \sum_{j=i+1}^n A_{ij} x_i x_j \quad (20)$$

which is summation of the excess Gibbs energy of each binary system in the multicomponent system. The activity coefficient of each component is thus calculated as in the following equation:

$$RT \ln \gamma_i = -g^E + \sum_{j=1, j \neq i}^n A_{ij} x_j \quad (21)$$

The presence of a single A parameter per component pair indicates the assumption that the interactions between two species in a mixture are symmetrical, that is, the interactions between species 1 and 2 in a 1:9 mixture are the same in a 9:1 mixture of the same two species, which is unlikely to be true in a crystalline system made up of TAGs of different FA chain lengths, or TAGs with the same FAs but at different glycerol positions.

Given this, the 2-suffix Margules equation can be extended to the 3-suffix Margules to account for different A parameters in a binary system, as

$$\begin{aligned} g^E &= x_1 x_2 (A_{21} x_1 + A_{12} x_2) \\ \Rightarrow RT \ln \gamma_1 &= x_2^2 [A_{12} + 2(A_{21} - A_{12}) x_1] \\ \Rightarrow RT \ln \gamma_2 &= x_1^2 [A_{21} + 2(A_{12} - A_{21}) x_2] \quad (22) \end{aligned}$$

Extending this to a multicomponent system gives Equation (23). It must be noted that the extension of the 3-suffix Margules equation to a multicomponent system is based on the assumption that the contribution to g^E by any given i - j pair is the same as if the components were in a binary mixture and not in a multicomponent one, at the same relative concentrations. When $A_{ij} = A_{ji}$, Equations (22) and (23) reduce to Equation (17) and Equations (19)–(21).

$$\begin{aligned} g^E &= \sum_{i=1}^n \sum_{j=i+1}^n \left(A_{ij} \frac{x_j}{x_i + x_j} + A_{ji} \frac{x_i}{x_i + x_j} \right) x_i x_j \\ \Rightarrow RT \ln \gamma_i &= -g^E + \sum_{j=1, j \neq i}^n x_j \left(\frac{A_{ji} (x_i^2 + 2x_i x_j) + A_{ij} x_j^2}{(x_i + x_j)^2} \right) \quad (23) \end{aligned}$$

It must be noted that all of the above models are used to describe liquid mixtures. These models were nonetheless used by Wesdorp (Marangoni & Wesdorp, 2013; Wesdorp, 1990) to determine whether the 2-suffix and 3-suffix Margules equations can be applied to nonideal solid mixing. This was done for a number of different binary TAG systems, be they un/saturated and a/symmetric TAGs. A number of empirical phase diagrams of temperature versus mole fraction were plotted, and the Margules equations were fitted to this empirical data. The authors noted that given that the solidus data may be very inaccurate, the A parameters were fitted only to the liquidus data points. In most cases, it was the 3-suffix Margules equation that was found to be most suitable to predict the four different types (monotectic¹ with continuous solid solubility, eutec-

tic,² monotectic with partial solid solubility, and peritectic³ (Timms, 1984)) of phase diagrams.

Notwithstanding this, the determined A parameters from the 2-suffix Margules equation were then used to predict the SFC profile of a number of commercial fats in the β' polymorph by using the equations described above, with, in most cases, good agreement with the empirically measured SFC profile.

A similar approach was taken by Teles dos Santos et al. (2014) who used a Gibbs energy minimization model to determine the SFC profile of a number of binary fat blends before and after interesterification. Using similar principles to Wesdorp (Marangoni & Wesdorp, 2013; Wesdorp, 1990), the authors used the following equation:

$$\begin{aligned} \min G(n) &= \sum_{i=1}^{nc} n_i^{liq} RT \sum_{i=1}^{nc} \left(x_i^{liq} \ln x_i^{liq} \right) \\ &+ \sum_{i=1}^{nc} n_i^{sol} RT \sum_{i=1}^{nc} x_i^{sol} \left(\frac{\Delta H_m}{R} \left(\frac{1}{T} - \frac{1}{T_m} \right) \right. \\ &\left. + \ln (\gamma_i^{sol} x_i^{sol}) \right) \quad (24) \end{aligned}$$

where n and x are the number of moles and the mole fraction of TAG i in the sol(id)/liq(uid) phase, respectively, γ was determined from the 2-suffix Margules equation, using A values as given by Wesdorp, whereas T_m and ΔH_f values were obtained from the Zéberg-Mikkelsen and Stenby (1999) and Wesdorp (1990) models when empirical values were not available.

Using the Gibbs free energy method gives a lot of flexibility to anyone looking at developing a blend of fats and oils to achieve a specific SFC profile, as it can be applied to more than just a binary system or a system made up of only a few TAGs. Similar to Wesdorp (1990) and Rocha and Guirardello (2009) (who, however, only applied similar theory to binary TAG systems), the SFC at different temperatures for a given blend is calculated by finding the distribution of molecules in the liquid and solid phases that minimizes the Gibbs free energy (G) (Equation 24). Given that all terms, except n and x (which can easily be expressed in terms of n), are known or are calculated from other models (such as the value of γ), the minimum value of G can be determined by varying the values of n for each TAG in each phase, thus determining the SFC at any given temperature.

¹ A monotectic system is one where at a given ratio of a binary system the mixture is either completely solid, is a mixture of a solid + liquid phase, or is completely liquid on increase in temperature.

² A eutectic system is one where at a specific ratio of a binary system, the melting point of the mixture is lower than the melting point of either pure component.

³ A peritectic point is the temperature at which, when cooling a system, a liquid and solid phase (e.g., a crystal in a specific polymorph) interact to form a different solid phase only (such as a different polymorph).

Given that the model to calculate the SFC of a binary blend of fats is based on the constituent TAGs of those fats and oils, and given the difference in thermodynamic properties of TAGs with the same FAs attached at different glycerol positions, the positional TAG composition profile of the different fats and oils must be known. The authors do, however, suggest that including only the TAGs, which make up at least 85% of the mass, should give a very good agreement with the empirically determined SFC curve. This is important given that the minor TAGs may not be individually quantified accurately when carrying out the positional TAG profile testing. When testing the model with various blends of different fats and oils, the results compared well with empirical values in most, if not all, cases, especially for the blends before interesterification (Teles dos Santos et al., 2013). A probable reason for this is the assumption made by the authors that the

3.3 | Most recent developments

A 2023 paper (Marangoni et al., 2023) proposes a new approach to predict the SFC. This study describes the development of a new nonideal equilibrium thermodynamics model (Equation 25), which takes into consideration not only the T_m and ΔH_f of each component TAG but also the entropy of mixing and the activity coefficient (γ) of a TAG in a solid medium. The latter two are used to calculate a freezing point depression, which is then integrated into an equilibrium expression for the melting of that TAG in such effective solid medium. As with other models, this model also assumes that the mixture of TAGs is found as a mixture of a liquid phase and a solid phase, with the solid phase being found in only one polymorphic form. The SFC content of the fat is then calculated by summing the amount of each TAG in the solid phase,

$$SFC (\%) = 100 \sum_{i=1}^n \left(\frac{[x_{t,i}]}{1 + \gamma_{ss,i} \exp \left(\frac{n_i \Delta H_{f,ns,i}^0}{R} \left(\frac{1}{T_{m,ns,i}} - \frac{R(\ln(\gamma_{ss,i} x_{t,i}) + x_{t,i} \ln(x_{t,i}) + (1-x_{t,i}) \ln(1-x_{t,i}))}{\Delta H_{f,ns,i}^0} - \frac{1}{T} \right) \right)} \right) \quad (25)$$

resulting FA positions in the TAGs after interesterification of the blends are completely random, based on the FA composition of the original blend, which may not be totally correct. This approach allows for extensive and rapid screening of different blends, that is, not only the use of different fats and oils but also at different ratios, which would save a lot of time and expense for product developers.

It has to be noted that while this approach is not new and has been used by others, such as Wesdorp (1990), the calculated SFC results did not always match empirical values closely. Teles dos Santos et al. (2013) compared the calculated values with empirical values published by Noor Lida et al. (2002) and some values differed by more than 23°C, indicating that this model may not always be suitable and may require some further refinement. In our view, this could be due to a number of factors, namely, inaccurate thermodynamic property values of the TAGs used, use of the thermodynamic properties in the wrong polymorph (the Teles dos Santos et al. paper does not specify the polymorph they calculated the SFC for), and/or the determination of a local minimum instead of a global minimum during the minimization of the Gibbs free energy.

where $x_{t,i}$ is the total mass of TAG i (i.e., a constant value), R is the universal gas constant (J/mol/K), $T_{m,ns}$ (K) and $\Delta H_{f,ns}$ (J/mol) are known (and constant), $\gamma_{ss,i}$ and n_i are the solid state activity coefficient and cooperativity index of TAG i (both constants), and T (temperature) is the only variable (K). The values for the activity coefficients γ and the cooperativity index n were fitted from eight different SFC profiles; however, a very good log-normal fit between n and γ was also determined (Equation 26), which could reduce the number of parameters that need to be determined even further, although at the moment this still remains an empirical relationship. Currently, there is no theory to calculate n using physicochemical principles, and this would require completely novel approaches to develop.

It must however be noted that if this n - γ relationship holds true and γ can be determined from other models as described in the previous subsection, ideally using nonempirical methods, that is, using models that are a function of only thermodynamic properties, then this model, as well as other models such as that outlined by others (Rocha & Guirardello, 2009; Teles dos Santos et al., 2013; Teles dos Santos et al., 2014), would in turn also ultimately be a function of only the thermodynamic properties (T_m and

ΔH_f) and the ratios of the component TAGs, obviating the requirement of any empirical parameter fitting.

$$n = \frac{9.1}{\gamma_{ss}} e^{-0.5 \left(\frac{\ln(\gamma_{ss}/6.70)}{1.59} \right)^2} \quad (26)$$

The relationship in Equation (26) is interpreted as follows: TAGs with a low activity coefficient (γ) interact with the solid medium the strongest, thus decreasing the connectivity between similar TAGs, whereas TAGs with a high γ value are likely to mean that these TAGs interact more strongly with similar TAGs, resulting in larger domains of a single-type TAG. In the median γ range, the TAGs would have optimal dispersion and interaction between individual TAG domains in the solid state.

It is currently still unknown whether a solid made up of a mixture of TAGs is completely isomorphous, whether TAGs are grouped as domains, and, if so, how large these domains. A question is thus posed whether this cooperativity index is a representation of the size of a domain of a TAG in a solid mixture/solution with other TAGs.

The approaches proposed by Schaik (2023) and Marangoni et al. (2023) offer an advantage over the Gibbs free energy minimization approach in that they are much less computationally expensive and have an analytical solution. The Gibbs free energy minimization approach relies on the selection of an appropriate minimization algorithm, which may not always find the global minimum, and the outcome of which may be dependent on the starting point of the minimization, as well as the algorithm's parameters (such as step-size and termination threshold).

4 | CRYSTALLIZATION MODELS

4.1 | Empirical models

The modeling of the isothermal crystallization of fats has been covered in a 2003 review by Foubert et al. (2003), and, hence, this review will only mention the models described therein briefly. These models are the Avrami (Avrami, 1939; Avrami, 1940), modified Avrami (Khanna & Taylor, 1988; Ng, 1975), Gompertz models, aggregation and flocculation models applied to crystallization (Berg & Brimberg, 1983), and their own Foubert model (Foubert et al., 2002).

The Avrami model (Avrami, 1939; Avrami, 1940) is one of the most widely used models used to describe fat crystallization kinetics, even though it was initially developed for metals (Foubert et al., 2003). In this model, the kinetics are governed by the number of growth nuclei, which can increase linearly with time (sporadic nucleation) or are formed mostly at the beginning of the liquid-to-crystal transformation process (instantaneous nucleation). The modified Avrami model (Khanna &

Taylor, 1988; Ng, 1975) is similar to the Avrami model, where the parameters have been rearranged. Foubert et al. stated that this changed the Avrami constant k from an m th-order complex constant to a first-order rate constant, even though crystallization is not a first-order process.

The Gompertz model, or Gompertz function, is a well-known mathematical description commonly used to describe biological processes. A reparameterized form of the equation (Zwietering et al., 1990) has, however, been used in a few studies to describe fat crystallization kinetics (Kloek et al., 2000; Vanhoutte et al., 2002). Berg and Brimberg (1983) showed that mathematical models describing the aggregation and flocculation of colloids also applied to fat crystallization, although Foubert et al. (2003) claimed that this is the only instance that they know of where these models have been applied to fats.

In contrast to the other models, the Foubert et al. (2002) given as a differential equation describing crystallization as a first-order forward reaction and an n th order reverse reaction. The authors state that, due to the differential form of the equation, the model can be used under dynamic temperature conditions, while having the advantage of having an analytical solution under isothermal conditions, facilitating parameter estimation (Foubert et al., 2002). The authors show that the Gompertz and Foubert models always perform better than the Avrami model, that is, the fitted curve is always closer to the empirically determined points, and the Foubert model performs better than the Gompertz model in most cases. The Foubert model also has the added advantage of being able to better fit different asymmetries.

This model was extended by the same group to describe two-step isothermal fat crystallization, a phenomenon that can occur due to polymorphism or the crystallization of different fractions (Foubert et al., 2006). This model was based on the assumption of the presence of an isosbestic point,⁴ which in this case involved a first crystallization step from melt to the α polymorph and a second step where the α polymorph recrystallized to the β' polymorph for cocoa butter and milk fat fractions.

4.2 | Thermodynamic and kinetic approaches to modeling crystallization

All of these models, however, are empirical models, which require experimental data to be able to estimate the

⁴ An isosbestic point is a point on a plot where all overlaid traces (in this case of SAXS diffraction patterns of cocoa butter at 20°C at increasing time points) converge. Such an isosbestic is indicative of a change from one polymorph to another without a change in the total volume.

parameters used in the model equations. A 2002 paper by Los et al. (2002) describes a kinetic crystallization model of a multicomponent system based on the pure-component melting enthalpies and temperatures and their excess energy parameters, that is, based on the thermodynamic properties and not on empirical parameters. Kinetic crystallization in mixed systems can be very complex, with multiple processes occurring, including nucleation, kinetic segregation, and diffusion, along with polymorphic changes and phase separation. To overcome this, the authors make two main assumptions: that the temperature and the composition of the liquid phase are homogenous, which they state is reasonable in a stirred fat system. Moreover, they state that thermodynamic models, where the final state is predicted by minimizing the Gibbs free energy of the system (such as those described in the previous chapter), reflect the most stable state of a multicomponent system, where any solid phase is completely homogenous. However, due to the very slow diffusion rates in solid phases, this thermodynamic, homogenous state is never reached during a finite time, and, hence, the final state is a metastable and non-homogenous solid phase. This, thus, makes a kinetic approach to crystallization a reasonable one (Los et al., 2002).

This kinetic model represents the crystallization evolution as crystallization curves, showing the growth rate and the changing liquid and solid compositions as a function of the increasing solid fraction. These curves show that significant inhomogeneity can occur in the solid phase, especially when this is composed of components with small excess energy parameters, that is, highly miscible components. This results in a smaller, kinetically predicted final solid fraction when compared to the equilibrium prediction, with the difference between predictions increasing with increasing solid fraction and component miscibility (Los et al., 2002). It must be noted that this work, along with work by others, is mentioned in the 2006 review by Himawan et al. (2006), which focuses on the thermodynamic and kinetic aspects of fat crystallization from melts.

5 | MOLECULAR DYNAMICS SIMULATIONS APPLIED TO TAGS

As discussed by Pink (2018), molecular dynamics (MD) is probably the best technique to study the structure and dynamics of food systems, such as TAGs and fats, at the nanoscale. MD concerns itself with the study the interaction of atoms and the weak physical interactions that influence this, not with chemical reactions, where covalent bonds are formed or broken. These interactions occur at a timescale that is much longer than the electronic

“motion,” and hence an average electronic distribution can be assumed. Thus, using *ab initio* techniques such as Density Functional Theory (a quantum mechanical [QM] modeling technique) or Car-Parrinello MD (a type of MD that calculates electronic interactions between atoms using QMs rather than empirical forcefields) is generally considered to be unnecessary (Pink, 2018). This paper discusses past and current MD studies on TAGs.

5.1 | Early attempts at modeling TAGs

One of the first papers published concerning simulations of TAG behavior is the 1994 paper by Yan et al. (1994). This study focused on determining the conformational and electrostatic properties of the TAGs by using semiempirical quantum mechanics and molecular mechanics (QM/MM). The TAGs studied in this case were trilaurin (1,2,3-tridodecanoyl-*sn*-glycerol), tridecyl 1,2,3-propanetricarboxylate, and five fully saturated mixed short-and-long-chained TAGs. The simulations were carried out using QUANTA/CHARMM molecular modeling and SPARTAN molecular orbital software, with all the simulations being carried out in the gas phase, with the goal being to determine the reactivities of the different TAGs toward lipase-mediated hydrolysis (Yan et al., 1994). Unsurprisingly, given the increased computational effort required compared to MD, this is the only known study where pure TAGs were simulated using a combination of QM/MM.

5.2 | Atomistic simulations

A 2002 study by Chandrasekhar and van Gunsteren (2002) evaluated six different GROMOS forcefield parameter sets to determine which of these simulated the structural and dynamic features of TAGs best. The study was done as, as per the authors' discussion, the parameterization of MD forcefields for TAGs is particularly challenging due to the polymorphic behavior of such lamellar systems, with the different polymorphs existing within a small temperature and density range. In addition, the existence of the different polymorphs is due to a number of variables, and, hence, the forcefield parameters have to be parameterized and tested very carefully in order to ensure that the simulations reproduce TAG behavior correctly. Forcefields that were parameterized for denser, or aqueous, systems had proven unsuitable as they resulted in unrealistic tilting of the chains (Chandrasekhar & van Gunsteren, 2002). The unsuitability of various forcefields to TAGs was found to be true by a number of different studies, as discussed in this section.

The Chandrasekhar and van Gunsteren study was on double layers of pure trioctanoin (1,2,3-trioctanoyl-*sn*-glycerol) in the α phase, that is, a nonaqueous system of the least thermodynamically stable polymorph of this TAG. The parameter sets focused on in this study were the 43A2 (Schuler & Van Gunsteren, 2000) and five variants of the 45A3 (Schuler, Daura, & van Gunsteren, 2001) GROMOS parameter sets. The five 45A3 parameter sets tested were as follows:

- the standard 45A3 parameter set,
- the 45A3 set with increased partial charges at the glycerol ester group,
- the 45A3-45 set (with increased ester carbon radius),
- the 45A3-45 \times 12 set (with variations on the ester carbon and united tetrahedral carbon radii), and
- the 45A3-45 \times 12 set with increased partial charges at the glycerol ester group.

The authors showed that all the six parameter sets retained the α polymorph as evaluated by the average cross-sectional area per chain (A_c), which they describe as a better parameter to use to assess phase behavior than volume or density. However, there were some notable differences in the results, namely, that the 45A3 parameter sets gave significantly better results when compared to the 43A2 parameter set and the unmodified 45A3 parameter set yielding the best results overall. This was highlighted by the fact that the 43A2 parameter set caused the TAG system to remain in a rigid and close packed system, which forced the system to tilt in a conformation that is known experimentally to be disallowed. On the other hand, after equilibration, the unmodified 45A3 parameter set retained the TAG system in a chair-like conformation (which in this case is referring to the general form of the molecule rather than the relative positioning of the chains) and the calculated A_c was very close to that expected. In addition, the total number of *trans* conformations of the alkyl chains compared well to empirical data, while no molecular tilt was observed.

The results obtained from the modified 45A3 parameter sets did not vary widely; however, when increasing the partial charges in the glycerol ester groups to those given by Chiu et al. (1995), there were significant changes in the volume of the box due to the different attractive and repulsive forces between the molecules, while the parameter sets with modified carbon radii gave rise to an increase in the box size as well as a reduction in the number of *trans* conformations, which was below that found experimentally. The authors concluded that the 45A3 parameter set was thus regarded as giving satisfactory results in simulating the properties of TAGs (Chandrasekhar & van Gunsteren, 2002). This paper highlighted the sensitivity of TAG simu-

lations to the forcefield used and can be considered to be of a seminal nature for MD simulations of TAGs, as a number of other studies published since then that describe MD simulations of TAGs have used the GROMOS96 forcefield, or variations of it, for their simulations.

A Masters thesis published in 2010 (Szewczyk, 2010) focused on the MD simulations of TAGs, with the aim of the study being to capture the first phase of the liquid-to-crystalline transformation of a pure TAG system. This work was based on the Chandrasekhar and van Gunsteren (2002) study, using the GROMOS96 forcefield for their MD simulations. The parameter subset chosen in this study was the 53A5 set (Oostenbrink et al., 2004), which is a refinement of the 45A3 parameter set (Schuler et al., 2001). This work focused on tripalmitin (1,2,3-tripalmitoyl-*sn*-glycerol) and tristearin (1,2,3-tristearoyl-*sn*-glycerol), that is, fully saturated and symmetric TAGs. The same study also investigated the use of a coarse-grained (CG) forcefield, in this case the Martini 2 forcefield (Marrink et al., 2007). The most successful results were those obtained with the GROMOS forcefield, with which densities close to the experimental value were obtained, whereas the results with the Martini 2 forcefield were not as good (<9% difference between experimental and simulated when using GROMOS versus 24% difference when using Martini 2), (Szewczyk, 2010) corroborating Chandrasekhar and van Gunsteren's claim that forcefields parameterized for non-TAG systems are unlikely to be suitable for pure TAG systems. This also highlights the issue that CG forcefields will usually give less accurate simulation results when compared to atomistic simulations if the CG forcefield has not been parameterized specifically to simulate for the property being investigated.

Two papers detailing the work in the groups of Marangoni and Pink published in 2012 (MacDougall et al., 2012) and 2014 (Razul et al., 2014) used MD simulations of TAGs to investigate the nanoscale characteristics and interactions of liquid oils to nanoplatelets of crystalline TAGs, such as the capacity of crystalline nanoparticles of tristearin to bind liquid triolein (1,2,3-trioleoyl-*sn*-glycerol). In both cases, the MD simulations were carried out using a variation of the GROMOS forcefield, which had been developed previously by Berger et al. (1997). The Berger forcefield uses the standard GROMOS forcefield parameters for all bonds, valence angles, and improper dihedrals, as well as for the dihedral angles in the headgroup region (the Berger study focused on dipalmitoylphosphatidylcholine [DPPC]). For the hydrocarbon chains, the Ryckaert-Bellemans potential is used, while for the nonbonded 1–4 interactions, the authors use the Lennard-Jones (LJ) as recommended by the optimized potentials for liquid simulations (OPLS) parameter set. The partial charges used in the main simulations of this

study were taken from the study by Chiu et al. (1995), which in this case gave simulated results that were very close to empirical results. It has however to be noted that the Berger study was on fully hydrated DPPC, that is, an aqueous system, that is, unlike that found in a hydrophobic fat.

5.3 | Finding the best forcefield for atomistic simulations

Briesen's group has published a number of papers on MD simulations of TAGs. Their studies, however, have been carried out using different forcefields. In a 2012 paper (Greiner, Reilly, et al., 2012) studying the effect of temperature and pressure on density and self-diffusion coefficients of monoacid TAGs, with the FA chains ranging from four to eighteen carbons, the parameters used by the authors were a combination of the forcefield developed by Nath and Khare (2001), Nath et al. (2001), Nath et al. (1998) for the aliphatic chains, while the glycerol backbone was modeled using the parameters given by Sum et al. (2003), collectively known as the NERD forcefield for TAGs. Although the results obtained showed the expected trends, it was hard to compare all the results with experimental data as this was not available at the time of publication.

Results presented at a 2012 conference (Greiner, Elts, et al., 2012) by the same group focused on the behavior of TAGs in high-pressure systems with the TAGs under study being *sn*-StOSt (1,3-distearoyl-2-oleoyl-*sn*-glycerol), *sn*-POSt (1-palmitoyl-2-oleoyl-3-stearoyl-*sn*-glycerol), and *sn*-POP (1,3-dipalmitoyl-2-oleoyl-*sn*-glycerol), that is, the main three TAG components of cocoa butter. In this case, they again used the NERD forcefield, with the authors again reporting the expected qualitative trend (when comparing to similar published data for cocoa butter; Greiner, Elts, et al., 2012) when plotting melting pressure against melting temperature for the three TAGs.

In a 2014 study (Greiner et al., 2014), the same group modeled the interaction of a 1,2-dilinoleoyl-phosphatidylcholine molecule (a key component of lecithin) with a sucrose crystal at a sucrose-cocoa butter interface, the latter being modeled as a specific mixture of *sn*-StOSt, *sn*-POSt, and *sn*-POP. This system was chosen as a model system for chocolate conching. In this case, the authors used the General Amber Forcefield (Wang et al., 2004), which the authors state was chosen given the fact that it was designed to cater for a wide variety of functional groups with the interaction parameters being readily available and tested for similar systems. The authors determined the simulations to be successful, with the surfactant molecule detaching from the sucrose

crystal face in stages, first one FA chain at a time, followed lastly by the choline headgroup, with the main limiting factors being the computational power and time needed with increasing system size and time scale (Greiner et al., 2014).

A 2018 study investigated the eutectic behavior of a binary mixture of tripalmitin and tristearin both empirically and computationally (Pizzirusso et al., 2018). The simulations for this study were carried out using the NERD forcefield, as an evaluation of four different forcefields, namely, the united atoms forcefields GROMOS96 and NERD and the all-atom forcefields OPLS and Large-OPLS, led the authors to the conclusion that at 293 K, the NERD forcefield gave the best agreement between the simulated and experimental crystal lattice parameters and crystal density for both TAGs. The authors also observed that on simulating the heating of the pure crystals in the β polymorph, the simulated crystal-to-liquid transition temperature was 35 K higher than the empirical value in both cases, with the empirical 5 K difference between the tripalmitin and tristearin melting points being reproduced computationally. The authors ascribed this 35 K offset to the approximation of the united atoms model, where the hydrogens are not considered independently but are part of the alkyl group. The binary mixtures in this study were modeled by starting with a pure tristearin crystal in the β polymorph and then randomly replacing a specific number of tristearin molecules with tripalmitin molecules. The conclusions of the study allowed for a molecular explanation of the eutectic phenomenon of the tripalmitin/tristearin binary mixtures, with the simulations agreeing with empirical results in identifying a mole fraction of 0.7 tripalmitin as the binary mixture with the lowest melting point (Pizzirusso et al., 2018).

Most of the studies described in this section were carried out on fully saturated monoacid TAGs, which, while simple, are not the most common TAGs found in nature. The applicability of the NERD forcefield as used by Briesen's group (Greiner, Elts, et al., 2012; Greiner, Reilly, et al., 2012) and Pizzirusso et al. (2018) and the GROMOS96 forcefield (with the 53A5 parameter set) were investigated by Cordina et al. (2021), who showed that this forcefield did not give good results when used for the simulation of crystalline monounsaturated TAGs, such as *sn*-POSt, *sn*-POP, and *sn*-StOSt when compared to empirical measurements such as lattice dimensions and density. The authors thus modified the NERD forcefield, namely, scaling the 1–4 electrostatic interactions of the forcefield, enabling a much better reproduction of the crystalline (including of different polymorphs of the same crystalline TAGs) and melted densities of unsaturated TAGs, as well as the lattice dimensions.

5.4 | From atomistic to coarse-grained simulations

A significant body of work relating to the MD simulations of TAGs has come from Milano's group. A 2009 doctoral thesis by Brasiello (2009) focused on the atomistic and CG MD simulations of tridecanoin (1,2,3-tridecanoyl-*sn*-glycerol). The atomistic simulations focused on determining the density change with temperature of the system, the radial distribution function (RDF) of the nonbonded interactions, the mean squared displacement of the system with time, and the viscosity of the system as a function of temperature. All these simulations were carried out using the GROMOS96 forcefield, with the author stating that they used the forcefield as described by Chandrasekhar and van Gunsteren (2002); however, they do not define which exact parameter set they used.

The density and viscosity were compared with available experimental data and found to be in close agreement. The computed self-diffusivity value, obtained from the mean squared displacement calculations, was of the same order of magnitude as liquid water, and in the absence of any experimental value, it was thus judged to be acceptable given that the simulations were performed on a liquid system. The carbon-carbon RDF showed a curve with a number of high peaks, typical of a liquid system where the FA chains have high flexibility and can thus interact, whereas the FA chain carbon-ester group RDF was much flatter, confirming that the ester groups are not being influenced by the FA chains.

The same group then developed a custom CG forcefield from the united atom simulations carried out on tridecanoin. The author claims that, to their knowledge, there is no literature describing CG models of TAGs and that the Martini 2 forcefield (Marrink et al., 2007) is inadequate for this purpose, as evidenced by a comparison of the distribution functions of bond angles and bond lengths between the GROMOS96 united atom results and the Martini 2 results, with the author showing that the bond lengths and angles are less stiff when using the Martini 2 forcefield (Brasiello, 2009). The RDFs from the Martini 2 forcefield also show higher nonbonded interactions when compared to the results obtained when using the GROMOS96 forcefield. The group thus developed a CG forcefield for TAGs where one glycerol carbon plus the ester group are considered to be one CG bead (distinguishing between the central and terminal glycerol positions), whereas the other beads are formed of three methylene/methyl groups, giving three bead types in total (Figure 3a). The coarse graining was improved in later publications as explained in Table 2.

In developing the CG forcefield, the author chose a harmonic potential for the two-body bonded potential, thus reducing the computational effort as it allows for the def-

inition of only two parameters instead of three, with the same being done for three-body bonded potentials. No four-body bonded potentials are defined, with the author justifying this approach because the dihedral distributions of the centers of mass of the groups represented in the CG model were completely random in the atomistic simulations (Brasiello, 2009). This holds true for a completely saturated system such as tridecanoin, given the full rotational freedom of the saturated methylene and methyl groups, but might not hold true for an unsaturated system such as an oleic chain (an 18-carbon chain with a *cis* double bond at C-9). As for two-body nonbonded interactions, the author used LJ 12-6 potentials.

The bonded parameters were determined by trial and error in such a way that the length and angle distributions overlapped with those obtained from the atomistic simulations. Given that, in the interests of computational efficiency, a harmonic oscillator model was chosen, the distributions were not always achieved perfectly as, for example, bimodal distributions observed from the atomistic simulations could only be reproduced as monomodal distributions. Notwithstanding this, the author argued that the distributions were still in quite good agreement. The two nonbonded LJ parameters were also determined by trial and error, while the mass was a simple summation of the mass of the atoms in each bead and the charge was set as zero given the overall neutral nature of each bead. It is, however, in our view that this is not quite correct. Although the glycerol-ester beads were distinguished on the basis of having a different mass (with the central bead grouping having one hydrogen atom less than the terminal beads), the FA chain beads should also be distinguished as the terminal chain bead is 1 atomic mass unit heavier.

In this case, the LJ parameters were fit so that the density of the box and the RDFs when using the CG model matched those obtained from the atomistic simulations. The RDFs obtained in this case showed a steeper growth than those from the atomistic simulations with the author attributing this to the fact that even though, given the coarse-graining, a "softer" nonbonded potential could be used, they still decided to use the LJ 12-6 potentials making the model less specific and thus more flexible for future applications. The author also notes that the LJ potentials between beads of different types differ slightly from those obtained when using the Lorentz-Berthelot mixing rules and are in fact corrected to give better overlapping RDFs (Brasiello, 2009).

This CG forcefield was then compared with the atomistic model and experimental data. Given that the CG model was developed from the data obtained from atomistic simulations at 446 K it was not surprising that the densities obtained from the atomistic and CG models at this temperature matched perfectly. The density

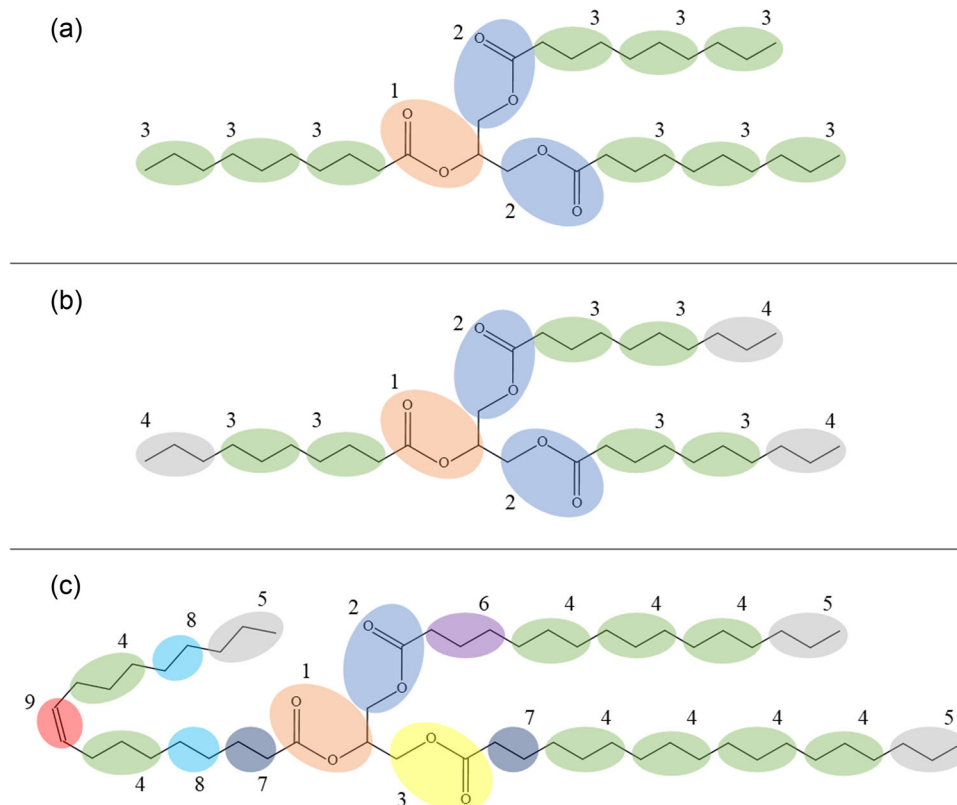


FIGURE 3 Evolution of the CG forcefields for triacylglycerides (TAGs). (a) Three bead forcefield developed for tridecanoin (Brasiello, 2009); (b) Four bead forcefield developed for tridecanoin (Brasiello et al., 2011); (c) Nine bead forcefield developed for unsaturated TAGs of varying length (Cordina et al., 2023b). In all cases, the numbers represent which beads are the same in the respective forcefield.

TABLE 1 Comparison of the various models to predict melting point and enthalpy of fusion of triacylglycerides (TAGs) [a]: Zacharis (1977), [b]: Timms (1978); [c]: Ollivon and Perron (1982); [d]: Marangoni and Wesdorp (2013), Moorthy et al. (2016), Seilert et al. (2021), Wesdorp (1990); [e]: Zéberg-Mikkelsen and Stenby (1999); [f]: Seilert and Flöter (2021).

Model	[a]	[b]	[c]	[d]	[e]	[f]
T_m	+	–	–	+	+	+
ΔH_f	–	+	+	–	+	+
ΔS_f	–	–	–	+	–	–
Saturated TAGs	+	+	+	+	+	+
Unsaturated TAGs	–	+	+	+	–	+
Asymmetrical TAGs	–	+	–	+	+	+
Polymorphs	$\alpha \beta' \beta$	$\beta' \beta$	$\beta' \beta$	$\alpha \beta' \beta$	$\alpha \beta' \beta$	$\alpha \beta' \beta$
Sub-polymorphs	–	–	–	–	–	–
$f(\text{individual fatty acid chains})$	–	–	–	+	+	+
Fatty acid position	–	–	–	+	+	+

TABLE 2 Table showing three different types of coarse-grained bead definition (Brasiello et al., 2011).

Bead	Model 1	Model 2	Model 3
<i>sn</i> -1 and <i>sn</i> -3 Glycerol carbon + ester group	Same bead type	Individual bead	Individual bead
<i>sn</i> -2 Glycerol carbon + ester group		Individual bead	Individual bead
$3 \times \text{CH}_2$ (fatty acid chain)	Same bead type	Same bead type	Individual bead
$2 \times \text{CH}_2 + 1 \times \text{CH}_3$ (fatty acid chain + terminal group)			Individual bead

calculated from simulations at other temperatures, however, diverged, with the plot of density against temperature obtained from the CG models being steeper than that from the atomistic model results. The atomistic density against temperature plot gradient mirrored that from experimental data, if slightly offset. The author, however, states that from calculations carried out, the results of the mean squared displacement suggest that the scaling factor between CG and atomistic simulations is 3, that is, every unit of CG simulation time is equivalent to three units of atomistic simulation time, meaning that simulations can be carried out over longer timescales by using CG modeling, even though the divergence between the atomistic and CG simulation results was observed. In the section looking at the phase transition of the TAG, the major drawback of this research is the fact that they cooled the system from 446 to 50 K using very rapid annealing rates, which meant that the molecules were mainly frozen in whatever conformation was adopted in the liquid state (Brasiello, 2009).

A 2011 paper (Brasiello et al., 2011) by the same group describes the development of the CG model for tridecanoin using the same principles but exploring the effect of defining different types of beads. Three different models were developed, as shown in Table 2. While the simulated density from all three models compared well with experimental data, it was clear that Model 3, that is, where the terminal glycerol carbons + ester groups were defined as a different bead type from the central bead and the terminal FA chain bead was also defined differently from the other chain beads (Figure 3b), gave the best results in terms of observing a phase transition from liquid to crystalline. When using Model 1 very little ordering of the molecules was observed when reducing the temperature, whereas Model 2 showed weak molecular aggregations. Model 3, however, showed a clear crystal transition on cooling from 446 to 200 K, with the glycerol-ester beads assembling with each other to form planes. The resulting crystal was determined to be in the α phase given the hexagonal packing of the molecules with no angle tilt, whereas the interchain distance was close to the experimental value for this polymorph (Brasiello et al., 2011). It is not clear from the paper whether the crystallization into the α polymorph is a consequence of the very low temperatures to which the system is cooled to or the CG model or both. Also, given the chain length and saturation of the FA chains in this study, with nine saturated carbons on each glycerol carbon (apart from the carbonyl carbon), defining the bead size and type was straightforward given that each bead type contained three carbons.

A collaboration between the Marangoni and Milano groups looked at the interactions of tripalmitin and tristearin as pure systems as well as a binary mixture

(Pizzirusso et al., 2015). The same CG model was used, this time being validated for the liquid-to-solid phase transition of pure tripalmitin and tristearin. The crystallization of a binary mixture of the TAGs resulted in the α polymorph (Pizzirusso et al., 2015), although this could be due to the fact that the simulations were cooled down rapidly from 446 to 175 K. The solid-to-liquid phase transition was reproduced qualitatively, that is, the same trend in melting point change was observed with changing tripalmitin/tristearin ratios as that obtained empirically; however, the computed values had an offset of around 90 K less than the empirical values. This study was characterized by significantly long simulation times, in some cases up to 100 μ s, although this was probably not required given that equilibrium was generally reached in a shorter timescale.

5.5 | Refining coarse-grained forcefields for TAGs

The Brasiello et al. (2011) paper uses four types of CG beads (Figure 3b), which was sufficient to describe tridecanoin. In the case of other TAGs, such as *sn*-POST, which has a different number of carbons in the different FA chains, this CG mapping is insufficient, as exemplified by the 15 saturated carbons in the palmitic chain and 17 saturated carbons in the stearic chain (excluding the carbonyl carbon of the FA chains, which is part of another CG bead). Thus, for a TAG such as *sn*-POST, bead definition would necessarily have to be a mixture of two and three carbon beads. This is further complicated by the presence of the *cis*-alkene group in the oleic chain, which would require the definition of a further separate bead type for the alkene group itself. As stated by Brasiello et al., the definition of different types of beads does not increase computational time if the number of beads is kept the same; however, it does lead to a significant improvement of the model (Brasiello et al., 2011).

This is the approach taken by Cordina et al. (2023b), who have developed the coarse-grained interchangeable triacylglyceride-optimized (COGITO) CG forcefield for TAGs which allows for the simulation of saturated and monounsaturated FA chains of varying length by parameterizing nine different CG beads; three for the different glycerol-ester bead types and a number of two or three hydrocarbon beads, depending on their position in the FA chain, including a specific bead for the alkene to allow for simulation of the oleic chain (Figure 3c). This CG mapping allows for a higher flexibility in simulating different TAGs including FA chains which vary by only two carbons, such as palmitic and stearic chains. In their study, the authors parameterized the various beads using a combination of bottom-up and top-down approaches. The bonded

parameters were based on their previous UA work (Cordina et al., 2021) (bottom-up), whereas the nonbonded parameters were determined by changing the parameters to fit a set of macroscopic measurements, such as density and lattice measurements (top-down). Given the number of LJ parameters that needed to be determined (in this case, eighteen) and the coupled nature of nonbonded potentials, the parameters were optimized using Bayesian Optimization, which allowed for simultaneous parameter estimation. The authors show good agreement of simulated crystalline and melted densities with empirical measurements, including for TAGs, which were not used to parameterize the forcefield, indicating the applicability of the forcefield. In addition to this, the authors also showed good agreement between the UA and CG RDFs, as well as being able to reproduce the trends, if not the magnitude, of the enthalpy of fusion and enthalpy of vaporization of various TAGs, despite not parameterizing against these metrics (Cordina et al., 2023b).

This paper was followed by another study by the same authors testing and showing the applicability of the COGITO forcefield to determine the melting points of pure TAG crystals. The authors employed a direct heating simulation method of pure TAG crystals with void defects, which enabled the accurate determination of the melting points of both short- and long-chain TAGs, as well as unsaturated and saturated TAGs (Cordina et al., 2023a). This study again used the COGITO forcefield on TAGs, which had not been used for initial forcefield parameterization, further testing the robustness of the forcefield.

The most recent paper by this group has extended this methodology further to binary systems of *sn*-POSt, *sn*-POP, and *sn*-StOSt (Cordina et al., 2023c). Using similar methodology as in their previous paper to determine the melting point of a single TAG-type crystal (Cordina et al., 2023a), the COGITO forcefield was tested to determine whether it could be used to determine the nonlinear behavior of such binary systems. The authors showed that, although the simulated melting points of the binary mixtures at various ratios were generally found to be lower than those determined empirically, the overall nonlinearity of the systems was reproduced well, such as the eutectic point of *sn*-POP/*sn*-POSt at a 50:50 ratio and *sn*-POP/*sn*-StOSt at a 80:20 ratio (Cordina et al., 2023c).

In summary, this chapter highlights the nascent stage of MD simulations research for TAGs and fats. Most of the early studies focused on fully saturated systems with only one type of FA, and it is only very recently that research has focused on the simulations of both crystalline and liquid asymmetric, unsaturated TAGs, that is, TAGs that are more commonly found in natural fats and oils. This has been done through the refinement and development of new forcefields. These have so far, however, been applied

to simple or model TAG systems and have not yet been applied to the simulation of more realistic fat systems with their multitude of different TAGs. This is the next step that should be undertaken to explore the full possibilities that MD can offer in this field. Until this is achieved, it will be harder for the food industry to apply this modeling technique to real-world problems, such as rheology and crystallization.

6 | CONCLUSIONS

This review has covered a range of different mathematical and computational models for TAGs and fats. This is an area of ongoing research, as evidenced by a number of papers that have been published over the past few years, highlighting the importance of the field in the food industry.

Although the applicability of models predicting individual TAG properties may be of limited use to the food industry when taken on their own, these find use in other models predicting fat properties, which could be of great use, such as in the prediction of solid-liquid equilibria. The implementation of such models by food companies to screen fats or even design the TAG composition of novel fats to achieve the desired physical properties should not be overly onerous, and any investment in implementing the models would be recouped many times over from the time and expense saved from carrying out empirical testing.

One thing to note here is that most, if not all, of the mathematical models discussed make use of empirically estimated parameters. This means that for the models to be implemented, some empirical data is still required, which can go counter to the rationale of using mathematical models in the first place, although we do acknowledge that most models require a degree of empirical data to be parameterized correctly. It will thus be of great value if purely first-principles models can be developed that can determine the properties of TAGs and fats without the need of empirical data. Another approach that can be taken is to investigate the “coupling” of different mathematical models to circumvent the requirement of empirical data to estimate a model’s parameters.

With ever-increasing computing power, modeling and simulation of fats and TAGs will only increase in use. This is especially relevant to MD simulations, which can be very computationally hungry. This is an area that requires more research, especially in the field of unsaturated TAGs, on which, while being very abundant in nature, there are only a few papers being published on this topic. This field can be considered to be still at a very early stage with not many publications being available. Given the computational resource required by MD simulations,

especially atomistic simulations, future research could focus on determining the representative elementary volume (REV) (i.e., the smallest number of molecules required) to be able to reproduce macroscopic behavior accurately. Whether the REV would be different for different applications would need to be determined, but having this kind of information would be of great benefit to researchers. This would enable such researchers to execute the most computationally efficient simulations while still getting accurate results, which would allow for the simulation of complex TAG systems (i.e., fats) over timescales that are representative of macroscopic phenomena. As an example, observing crystallization is known to be very difficult when using MD, mainly because this can occur over timescales that are not computationally feasible to reach. By minimizing the number of molecules that are simulated, this could then become achievable in a reasonable simulation time.

AUTHOR CONTRIBUTIONS

Robert J. Cordina: Writing—original draft; conceptualization. **Beccy Smith:** Writing—review and editing; conceptualization; supervision. **Tell Tuttle:** Writing—review and editing; conceptualization; supervision.


ACKNOWLEDGMENTS

The authors thank Mondelēz International for supporting this work.

CONFLICTS OF INTEREST STATEMENT

The authors declare no conflicts of interest.

ORCID

Robert J. Cordina  <https://orcid.org/0000-0003-2538-543X>

REFERENCES

- Augusto, P. E. D., Soares, B. M. C., Chiu, M. C., & Gonçalves, L. A. G. (2012). Modelling the effect of temperature on the lipid solid fat content (SFC). *Food Research International*, 45(1), 132–135. <https://doi.org/10.1016/j.foodres.2011.10.026>
- Avrami, M. (1939). Kinetics of phase change. I General theory. *The Journal of Chemical Physics*, 7(12), 1103–1112. <https://doi.org/10.1063/1.1750380>
- Avrami, M. (1940). Kinetics of phase change. II Transformation-Time relations for random distribution of nuclei. *The Journal of Chemical Physics*, 8(2), 212–224. <https://doi.org/10.1063/1.1750631>
- Bayés-García, L., Calvet, T., Àngel Cuevas-Diarte, M., Ueno, S., & Sato, K. (2013). In situ observation of transformation pathways of polymorphic forms of 1,3-dipalmitoyl-2-oleoyl glycerol (POP) examined with synchrotron radiation X-ray diffraction and DSC. *CrystEngComm*, 15(2), 302–314. <https://doi.org/10.1039/C2CE26522B>
- Ben Hassen, T., & El Bilali, H. (2022). Impacts of the Russia-Ukraine war on global food security: Towards more sustainable and resilient food systems? *Foods*, 11(15), 2301. <https://doi.org/10.3390/foods11152301>
- Berg, T. G. O., & Brimberg, U. I. (1983). Über die kinetik der fettkristallisation. *Fette, Seifen, Anstrichmittel*, 85(4), 142–149. <https://doi.org/10.1002/lipi.19830850402>
- Berger, O., Edholm, O., & Jaehnig, F. (1997). Molecular dynamics simulations of a fluid bilayer of dipalmitoylphosphatidylcholine at full hydration, constant pressure, and constant temperature. *Biophysical Journal*, 72, 2002–2013.
- Block, J. M., Barrera-Arellano, D., Figueiredo, M. F., & Gomide, F. A. C. (1997). Blending process optimization into special fat formulation by neural networks. *Journal of the American Oil Chemists' Society*, 74(12), 1537–1541. <https://doi.org/10.1007/s11746-997-0073-5>
- Brsiello, A. (2009). *Molecular dynamics of triglycerides: Atomistic and coarse-grained approaches* [Tesi di dottorato, Università degli Studi di Napoli Federico II, Naples, Italy]. <https://doi.org/10.6092/UNINA/FEDOA/1846>
- Brsiello, A., Crescitelli, S., & Milano, G. (2011). Development of a coarse-grained model for simulations of tridecanoin liquid–solid phase transitions. *Physical Chemistry Chemical Physics: PCCP*, 13(37), 16618–16628. <https://doi.org/10.1039/c1cp20604d>
- Chandrasekhar, I., & van Gunsteren, W. (2002). A comparison of the potential energy parameters of aliphatic alkanes: Molecular dynamics simulations of triacylglycerols in the alpha phase. *European Biophysics Journal*, 31(2), 89–101. <https://doi.org/10.1007/s00249-001-0196-9>
- Chiu, S., Clark, M., Balaji, V., Subramaniam, S., Scott, H. L., & Jakobsson, E. (1995). Incorporation of surface tension into molecular dynamics simulation of an interface: A fluid phase lipid bilayer membrane. *Biophysical Journal*, 69, 1230–1245.
- Cordina, R. J., Smith, B., & Tuttle, T. (2021). Reproduction of macroscopic properties of unsaturated triacylglycerides using a modified NERD force field. *Journal of Molecular Graphics & Modelling*, 108, 107996. <https://doi.org/10.1016/j.jmgm.2021.107996>
- Cordina, R. J., Smith, B., & Tuttle, T. (2023a). Triacylglyceride melting point determination using coarse-grained molecular dynamics. *Journal of Computational Chemistry*, 44(21), 1795–1801. <https://doi.org/10.1002/jcc.27128>
- Cordina, R. J., Smith, B., & Tuttle, T. (2023b). COGITO: A coarse-grained force field for the simulation of macroscopic properties of triacylglycerides. *Journal of Chemical Theory and Computation*, 19(4), 1333–1341. <https://doi.org/10.1021/acs.jctc.2c00975>
- Cordina, R. J., Smith, B., & Tuttle, T. (2023c). Predicting lipid eutectics using coarse-grained molecular dynamics. *Journal of Physical Chemistry B*, 127(47), 10236–10242. <https://doi.org/10.1021/acs.jpcc.3c06297>
- Culot, C., Norberg, B., Evrard, G., & Durant, F. (2000). Molecular analysis of the β -polymorphic form of trielaidin: Crystal structure at low temperature. *Acta Crystallographica. Section B, Structural Science*, 56(2), 317–321. <https://doi.org/10.1107/S0108768199014020>
- Devi, A., & Khatkar, B. S. (2016). Physicochemical, rheological and functional properties of fats and oils in relation to cookie quality: A review. *Journal of Food Science and Technology*, 53(10), 3633–3641. <https://doi.org/10.1007/s13197-016-2355-0>
- Dhaka, V., Gulia, N., Ahlawat, K. S., & Khatkar, B. S. (2011). Trans fats—Sources, health risks and alternative approach—A review.

- Journal of Food Science and Technology*, 48(5), 534–541. <https://doi.org/10.1007/s13197-010-0225-8>
- Ehlers, D. (2012). *Controlled crystallization of complex confectionery fats* [PhD thesis, ETH Zurich, Zürich, Switzerland].
- Eibl, R., Senn, Y., Gubser, G., Jossen, V., van den Bos, C., & Eibl, D. (2021). Cellular agriculture: Opportunities and challenges. *Annual Review of Food Science and Technology*, 12(1), 51–73. <https://doi.org/10.1146/annurev-food-063020-123940>
- Farr, W. E., Ghazani, S. M., & Marangoni, A. G. (2005). *Hydrogenation: Processing technologies*. John Wiley & Sons, Ltd. <https://doi.org/10.1002/047167849X.bio064.pub2>
- Foubert, I., Dewettinck, K., Janssen, G., & Vanrolleghem, P. A. (2006). Modelling two-step isothermal fat crystallization. *Journal of Food Engineering*, 75(4), 551–559. <https://doi.org/10.1016/j.jfoodeng.2005.04.038>
- Foubert, I., Dewettinck, K., & Vanrolleghem, P. A. (2003). Modelling of the crystallization kinetics of fats. *Trends in Food Science & Technology*, 14(3), 79–92. [https://doi.org/10.1016/S0924-2244\(02\)00256-X](https://doi.org/10.1016/S0924-2244(02)00256-X)
- Foubert, I., Vanrolleghem, P. A., Vanhoutte, B., & Dewettinck, K. (2002). *Dynamic mathematical model of the crystallization kinetics of fats*. Elsevier BV. [https://doi.org/10.1016/S0963-9969\(02\)00157-6](https://doi.org/10.1016/S0963-9969(02)00157-6)
- Garti, N., & Widlak, N. R. (2012). *Cocoa butter and related compounds: Challenges in food systems*. AOCS.
- Ghazani, S. M., & Marangoni, A. G. (2018). New insights into the β polymorphism of 1,3-palmitoyl-stearoyl-2-oleoyl glycerol. *Crystal Growth & Design*, 18(9), 4811–4814. <https://doi.org/10.1021/acs.cgd.8b00598>
- Ghazani, S. M., & Marangoni, A. G. (2023). New triclinic polymorph of tristearin. *Crystal Growth & Design*, 23(3), 1311–1317. <https://doi.org/10.1021/acs.cgd.2c01334>
- Glauben, T., Svanidze, M., Götz, L., Prehn, S., Jamali Jaghdani, T., Đurić, I., & Kuhn, L. (2022). The war in Ukraine, agricultural trade and risks to global food security. *Intereconomics*, 57(3), 157–163. <https://doi.org/10.1007/s10272-022-1052-7>
- Greiner, M., Elts, E., & Briesen, H. (2012). *Molecular dynamics simulations as a predictive tool for the behavior of fats in high-pressure processes* [Conference presentation]. 7th International Conference on Simulation and Modelling in the Food and Bio-Industry 2012, FOODSIM 2012, Freising, Germany.
- Greiner, M., Reilly, A. M., & Briesen, H. (2012). Temperature- and pressure-dependent densities, self-diffusion coefficients, and phase behavior of monoacid saturated triacylglycerides: Toward molecular-level insights into processing. *Journal of Agricultural and Food Chemistry*, 60(20), 5243–5249. <https://doi.org/10.1021/jf3004898>
- Greiner, M., Sonnleitner, B., Mailaender, M., & Briesen, H. (2014). Modeling complex and multi-component food systems in molecular dynamics simulations on the example of chocolate conching. *Food & Function*, 5(2), 235–242. <https://doi.org/10.1039/c3fo60355e>
- Gunstone, F. D. (2008). *Oils and fats in the food industry* (1. publ. ed.). Wiley-Blackwell. <https://doi.org/10.1002/9781444302424>
- Hildebrand, J. H. (1929). Solubility. XII. Regular solutions. *Journal of the American Chemical Society*, 51(1), 66–80. <https://doi.org/10.1021/ja01376a009>
- Himawan, C., Starov, V. M., & Stapley, A. G. F. (2006). Thermodynamic and kinetic aspects of fat crystallization. *Advances in Colloid and Interface Science*, 122(1), 3–33. <https://doi.org/10.1016/j.cis.2006.06.016>
- Khanna, Y. P., & Taylor, T. J. (1988). Comments and recommendations on the use of the Avrami equation for physico-chemical kinetics. *Polymer Engineering and Science*, 28(16), 1042–1045. <https://doi.org/10.1002/pen.760281605>
- Kloek, W., Walstra, P., & Vliet, T. (2000). Crystallization kinetics of fully hydrogenated palm oil in sunflower oil mixtures. *Journal of the American Oil Chemists' Society*, 77(4), 389–398. <https://doi.org/10.1007/s11746-000-0063-z>
- Los, J. H., van Enkevort, W. J. P., Vlieg, E., & Flöter, E. (2002). Metastable states in multicomponent liquid–solid systems I: A kinetic crystallization model. *The Journal of Physical Chemistry. B*, 106(29), 7321–7330. <https://doi.org/10.1021/jp025728b>
- MacDougall, C. J., Razul, M. S., Papp-Szabo, E., Peyronel, F., Hanna, C. B., Marangoni, A. G., & Pink, D. A. (2012). Nanoscale characteristics of triacylglycerol oils: Phase separation and binding energies of two-component oils to crystalline nanoplatelets. *Faraday Discussions*, 158, 425–433. <https://doi.org/10.1039/c2fd20039b>
- Marangoni, A. G., Ghazani, S. M., & Pensini, E. (2023). An entropy-centric equilibrium cooperative theory for the melting behavior of nonideal triacylglycerol mixtures. *Journal of the American Oil Chemists' Society*, 100(2), 107–122. <https://doi.org/10.1002/aocs.12669>
- Marangoni, A. G., & Wesdorp, L. H. (2013). Liquid–Multiple solid phase equilibria in fats: Theory and experiments. *Structure and properties of fat crystal networks* (pp. 260–437). CRC Press. <https://doi.org/10.1201/b12883-11>
- Margules, M. (1895). Über die Zusammensetzung der gesättigten dämpfe von mischungen. *Sitzungsberichte Der Kaiserliche Akademie Der Wissenschaften Wien Mathematisch-Naturwissenschaftliche Klasse II*, 104, 1243–1278.
- Marrink, S. J., Risselada, H. J., Yefimov, S., Tieleman, D. P., & de Vries, A. H. (2007). The MARTINI force field: Coarse grained model for biomolecular simulations. *The Journal of Physical Chemistry. B*, 111(27), 7812–7824. <https://doi.org/10.1021/jp071097f>
- Mensink, R. P., Sanders, T. A., Baer, D. J., Hayes, K. C., Howles, P. N., & Marangoni, A. (2016). The increasing use of interesterified lipids in the food supply and their effects on health parameters. *Advances in Nutrition (Bethesda, Md.)*, 7(4), 719–729. <https://doi.org/10.3945/an.115.009662>
- Moorthy, A. S., Liu, R., Mazzanti, G., Wesdorp, L. H., & Marangoni, A. G. (2017). Estimating thermodynamic properties of pure triglyceride systems using the triglyceride property calculator. *Journal of the American Oil Chemists' Society*, 94(2), 187–199. https://lipidlibrary.shinyapps.io/Triglyceride_Property_Calculator/
- Moorthy, A. S., Liu, R., Mazzanti, G., Wesdorp, L. H., & Marangoni, A. G. (2017). Estimating thermodynamic properties of pure triglyceride systems using the triglyceride property calculator. *Journal of the American Oil Chemists' Society*, 94(2), 187–199. <https://doi.org/10.1007/s11746-016-2935-1>
- Nath, S. K., Banaszak, B. J., & de Pablo, J. J. (2001). A new united atom force field for α -olefins. *The Journal of Chemical Physics*, 114(8), 3612–3616. <https://doi.org/10.1063/1.1343487>
- Nath, S. K., Escobedo, F. A., & de Pablo, J. J. (1998). On the simulation of vapor–liquid equilibria for alkanes. *The Journal of Chemical Physics*, 108(23), 9905–9911. <https://doi.org/10.1063/1.476429>
- Nath, S. K., & Khare, R. (2001). New forcefield parameters for branched hydrocarbons. *The Journal of Chemical Physics*, 115(23), 10837–10844. <https://doi.org/10.1063/1.1418731>

- Ng, W. L. (1975). Thermal decomposition in the solid state. *Australian Journal of Chemistry*, 28, 1169–1178. <https://doi.org/10.1071/CH9751169>
- Noor Lida, H. M. D., Sundram, K., Siew, W. L., Aminah, A., & Mamot, S. (2002). TAG composition and solid fat content of palm oil, sunflower oil, and palm kernel olein blends before and after chemical interesterification. *Journal of the American Oil Chemists' Society*, 79(11), 1137–1144. <https://doi.org/10.1007/s11746-002-0617-0>
- Novelli, E. (2016). Sustainability as a success factor for palm oil producers supplying the European vegetable oil markets. *Oil Palm Industry Economic Journal*, 16(1), 8–17.
- Ollivon, M., & Perron, R. (1982). Measurements of enthalpies and entropies of unstable crystalline forms of saturated even monoacid triglycerides. *Thermochimica Acta*, 53(2), 183–194. [https://doi.org/10.1016/0040-6031\(82\)85007-7](https://doi.org/10.1016/0040-6031(82)85007-7)
- Oostenbrink, C., Villa, A., Mark, A. E., & van Gunsteren, W. F. (2004). A biomolecular force field based on the free enthalpy of hydration and solvation: The GROMOS force-field parameter sets 53A5 and 53A6. *Journal of Computational Chemistry*, 25(13), 1656–1676. <https://doi.org/10.1002/jcc.20090>
- Peschar, R., Schenk, H., & van Mechelen, J. B. (2006). Structures of mono-unsaturated triacylglycerols. II. The β_2 polymorph. *Acta Crystallographica Section B*, 62(6), 1131–1138. <https://doi.org/10.1107/S0108768106037074>
- Pink, D. A. (2018). Modeling interactions in edible fats. In A. G. Marangoni (Ed.), *Structure-function analysis of edible fats* (2nd ed., pp. 197–240). AOCS Press. <https://doi.org/10.1016/C2017-0-00579-7>; <https://app.knovel.com/hotlink/toc/id:kpSFAEFE02/structure-function-analysis/structure-function-analysis?kpromoter=Summon>
- Pizzirusso, A., Brasiello, A., De Nicola, A., Marangoni, A. G., & Milano, G. (2015). Coarse-grained modelling of triglyceride crystallisation: A molecular insight into tripalmitin tristearin binary mixtures by molecular dynamics simulations. *Journal of Physics D: Applied Physics*, 48(49), 494004. <https://doi.org/10.1088/0022-3727/48/49/494004>
- Pizzirusso, A., Peyronel, F., Co, E. D., Marangoni, A. G., & Milano, G. (2018). Molecular insights into the eutectic tripalmitin/tristearin binary system. *Journal of the American Chemical Society*, 140(39), 12405–12414. <https://doi.org/10.1021/jacs.8b04729>
- Prausnitz, J. M., Lichtenthaler, R. N., & de Azevedo, E. G. (1999). *Molecular thermodynamics of fluid phase equilibria* (3rd ed.). Prentice Hall.
- Razul, M. S. G., MacDougall, C. J., Hanna, C. B., Marangoni, A. G., Peyronel, F., Papp-Szabo, E., & Pink, D. A. (2014). Oil binding capacities of triacylglycerol crystalline nanoplatelets: Nanoscale models of tristearin solids in liquid triolein. *Food & Function*, 5(10), 2501–2508. <https://doi.org/10.1039/C3FO60654F>
- Rocha, S. A., & Guirardello, R. (2009). An approach to calculate solid–liquid phase equilibrium for binary mixtures. *Fluid Phase Equilibria*, 281(1), 12–21. <https://doi.org/10.1016/j.fluid.2009.03.020>
- Schaink, H. M. (2023). Calculation of the solid fat content of vegetable fats using the Hildebrand equation. *Journal of the American Oil Chemists' Society*, 100(12), 929–944. <https://doi.org/10.1002/aocs.12724>
- Schirmer, C., Eibl, R., Maschke, R. W., Mozaffari, F., Junne, S., Daumke, R., Ottinger, M., Göhmann, R., Ott, C., Wenk, I., Kubishcik, J., & Eibl, D. (2022). Single-use technology for the production of cellular agricultural products: Where are we today? *Chemie Ingenieur Technik*, 94(12), 2018–2025. <https://doi.org/10.1002/cite.202200092>
- Schuler, L. D., Daura, X., & van Gunsteren, W. F. (2001). An improved GROMOS96 force field for aliphatic hydrocarbons in the condensed phase. *Journal of Computational Chemistry*, 22(11), 1205–1218. <https://doi.org/10.1002/jcc.1078.abs>
- Schuler, L. D., & Van Gunsteren, W. F. (2000). On the choice of dihedral angle potential energy functions for n-alkanes. *Molecular Simulation*, 25(5), 301–319. <https://doi.org/10.1080/08927020008024504>
- Seilert, J., & Flöter, E. (2021). A configurational approach to model triglyceride pure component properties. *European Journal of Lipid Science and Technology*, 123(10), 2100010. <https://doi.org/10.1002/ejlt.202100010>
- Seilert, J., Moorthy, A. S., Kearsley, A. J., & Flöter, E. (2021). Revisiting a model to predict pure triglyceride thermodynamic properties: Parameter optimization and performance. *Journal of the American Oil Chemists' Society*, 98(8), 837–850. <https://doi.org/10.1002/aocs.12515>
- Smith, K. W., Bhaggan, K., & Talbot, G. (2013). Phase behavior of symmetrical monounsaturated triacylglycerols. *European Journal of Lipid Science and Technology*, 115(8), 838–846. <https://doi.org/10.1002/ejlt.201300035>
- Sum, A. K., Bidy, M. J., de Pablo, J. J., & Tupy, M. J. (2003). Predictive molecular model for the thermodynamic and transport properties of triacylglycerols. *The Journal of Physical Chemistry B*, 107(51), 14443–14451. <https://doi.org/10.1021/jp035906g>
- Szewczyk, P. (2010). *Study of the phase behavior of triacylglycerols using molecular dynamics simulation* [MSc Thesis, University of Alberta, Edmonton, Alberta, Canada].
- Talbot, G. (2016). Developing food products for customers with low fat and low saturated fat requirements: Dairy and meat products. In S. Osborn & W. Morley (Eds.), *Developing food products for consumers with specific dietary needs* (pp. 107–128). Woodhead Publishing. <https://doi.org/10.1016/B978-0-08-100329-9.00006-2>; <https://www.sciencedirect.com/science/article/pii/B9780081003299000062>
- Teles dos Santos, M., Gerbaud, V., & Roux, G. A. C. L. (2013). Modeling and simulation of melting curves and chemical interesterification of binary blends of vegetable oils. *Chemical Engineering Science*, 87(14), 14–22. <https://doi.org/10.1016/j.ces.2012.09.026>
- Teles dos Santos, M., Gerbaud, V., & Le Roux, G. A. C. (2014). Solid fat content of vegetable oils and simulation of interesterification reaction: Predictions from thermodynamic approach. *Journal of Food Engineering*, 126, 198–205. <https://doi.org/10.1016/j.jfoodeng.2013.11.012>
- Timms, R. E. (1978). Heats of fusion of glycerides. *Chemistry and Physics of Lipids*, 21(1), 113–129. [https://doi.org/10.1016/0009-3084\(78\)90059-2](https://doi.org/10.1016/0009-3084(78)90059-2)
- Timms, R. E. (1984). Phase behaviour of fats and oils and their mixtures. *Progress in Lipid Research*, 23, 1–38. [https://doi.org/10.1016/0163-7827\(84\)90004-3](https://doi.org/10.1016/0163-7827(84)90004-3)
- Van Langevelde, A., Peschar, R., & Schenk, H. (2001). Structure of β -trimyristin and β -tristearin from high-resolution X-ray powder diffraction data. *Acta Crystallographica. Section B, Structural Science*, 57(3), 372–377. <https://doi.org/10.1107/S010876810001-9121>

- van Mechelen, J. B., Peschar, R., & Schenk, H. (2006). Structures of mono-unsaturated triacylglycerols. I. The $\beta 1$ polymorph. *Acta Crystallographica Section B*, 62(6), 1121–1130. <https://doi.org/10.1107/S0108768106037086>
- Vanhoutte, B., Dewettinck, K., Foubert, I., Vanlerberghe, B., & Huyghebaert, A. (2002). The effect of phospholipids and water on the isothermal crystallisation of milk fat. *European Journal of Lipid Science and Technology*, 104(8), 490–495. [https://doi.org/10.1002/1438-9312\(200208\)104:83.0.CO;2-U](https://doi.org/10.1002/1438-9312(200208)104:83.0.CO;2-U)
- Wang, J., Wolf, R. M., Caldwell, J. W., Kollman, P. A., & Case, D. A. (2004). Development and testing of a general amber force field. *Journal of Computational Chemistry*, 25(9), 1157–1174. <https://doi.org/10.1002/jcc.20035>
- Wesdorp, L. (1990). *Liquid-multiple solid phase equilibria in fats: Theory and experiments* [PhD thesis, TU Delft, Delft, The Netherlands].
- Yan, Z. Y., Huhn, S. D., Klemann, L. P., & Otterburn, M. S. (1994). Molecular modeling studies of triacylglycerols. *Journal of Agricultural and Food Chemistry*, 42(2), 447–452. <https://doi.org/10.1021/jf00038a039>
- Zacharis, H. M. (1977). A linear function for the melting behavior of lipids. *Chemistry and Physics of Lipids*, 18(2), 221–231. [https://doi.org/10.1016/0009-3084\(77\)90009-3](https://doi.org/10.1016/0009-3084(77)90009-3)
- Zagury, Y., Ianovici, I., Landau, S., Lavon, N., & Levenberg, S. (2022). Engineered marble-like bovine fat tissue for cultured meat. *Communications Biology*, 5(1), 927. <https://doi.org/10.1038/s42003-022-03852-5>
- Zéberg-Mikkelsen, C. K., & Stenby, E. H. (1999). *Predicting the melting points and the enthalpies of fusion of saturated triglycerides by a group contribution method*. Elsevier BV. [https://doi.org/10.1016/s0378-3812\(99\)00171-5](https://doi.org/10.1016/s0378-3812(99)00171-5)
- Zhang, L., Ueno, S., & Sato, K. (2018). Binary phase behavior of saturated-unsaturated mixed-acid triacylglycerols—A review. *Journal of Oleo Science*, 67(6), 679–687. <https://doi.org/10.5650/jos.ess17263>
- Zwietering, M. H., Jongenburger, I., Rombouts, F. M., & van 't Riet, K. (1990). Modeling of the bacterial growth curve. *Applied and Environmental Microbiology*, 56(6), 1875–1881. <https://doi.org/10.1128/aem.56.6.1875-1881.1990>

How to cite this article: Cordina, R. J., Smith, B., & Tuttle, T. (2024). Mathematical and computational modeling of fats and triacylglycerides. *Comprehensive Reviews in Food Science and Food Safety*, 23, e13316. <https://doi.org/10.1111/1541-4337.13316>